Property Determinants of Dextran:Polyethylene Glycol Adhesive Sealants

by

Tarek Shazly

B.S. Mechanical Engineering
Georgia Institute of Technology, 2001

M.S. Bioengineering
Georgia Institute of Technology, 2004

SUBMITTED TO THE DEPARTMENT OF MATERIALS SCIENCE AND ENGINEERING
IN PARTIAL FULFILLMENT OF THE REQUIREMENTS FOR THE DEGREE OF

MASTER OF SCIENCE IN MATERIALS SCIENCE AND ENGINEERING

AT THE

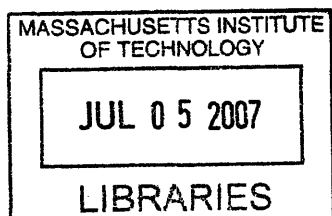MASSACHUSETTS INSTITUTE OF TECHNOLOGY

June 2007

Signature of Author: _____
Department of Materials Science and Engineering
May 15, 2007

Certified by: _____
Elazer R. Edelman
Thomas D. and Virginia W. Cabot Professor Professor of Health Science and Technology
Thesis Supervisor

Read by: _____
David Roylance
Professor of Materials Science and Engineering
Thesis Reader

Accepted by: _____
Samuel M. Allen
POSCO Professor of Physical Metallurgy
Chair, Departmental Committee on Graduate Students

Property Determinants of Dextran:Polyethylene Glycol Adhesive Sealants

Submitted to the Department of Materials Science and Engineering on May 15, 2007 in partial fulfillment of the requirements for Masters of Science in Materials Science and Engineering

Abstract

Internal surgical intervention necessitates the intentional wounding of tissue. In certain clinical procedures, the desired wound healing response requires the use of closure techniques, such as suturing or stapling of disjoined tissues. Risk factors associated with these techniques are largely attributed to the discrete nature of the mechanical forces arising in the tissues. Adhesive sealants can mitigate risk by imparting a continuous stress distribution to tissues upon closure, as opposed to destructive stress concentrations. A novel class of dextran:polyethylene glycol hydrogels are a potential alternative to the limited selection of available adhesive sealants. Multiple compositional variations are available for both the dextran and polyethylene glycol components, making a wide range of clinically relevant material properties achievable. Key material properties determining sealant efficacy include hydration and degradation in an aqueous medium, elastic modulus, adhesion strength to tissue, and biocompatibility. Relationships between these pertinent properties and available compositional variations are determined for dextran:polyethylene glycol materials. Gravimetric, mechanical and biological testing reveal the following compositional determinants of material properties in dextran:polyethylene glycol copolymers: constituent molecular complexity dictates material hydration and degradation, solid content dictates elastic modulus, available aldehyde groups dictate adhesion strength, and material solid content and reactive group ratio dictate induced cell proliferation and cytotoxicity. Knowledge of these property determinants facilitates development of an optimal dextran:polyethylene glycol material in a small bowel resection model for adhesive sealants, and furthers the understanding of these complex copolymers for other sealant applications. Generalization of the identified property determinants to other material classes provides a vehicle for advancement of adhesive sealant technologies.

Thesis Supervisor: Elazer R. Edelman
Title: Thomas D. and Virginia W. Cabot Professor
Division of Health Sciences and Technology

Acknowledgments

Table of Contents

List of Figures

List of Tables

Chapter 1: Introduction

1.1 Scientific Motivation: Adhesive Sealant Limitations

Soft tissue adhesive sealants are used in internal surgery as a means to attain homeostasis and withstand mechanical loads [1-4]. Particular sealant applications include repair of lacerations, filling of void spaces, and topical use to prevent dermal scarring [5, 6]. Although clinical outcomes of adhesive sealant applications are generally acceptable, available materials are limited by a lack of adhesion strength or tissue insult upon adherence [1, 7-9]. Commercially available fibrin sealants lose adhesion to tissue shortly after implantation, and have showed a dangerous tendency to pool bacteria and debris at a wound site [10, 11]. More chemically reactive sealants, such as cyanoacrylate glues, are also available and provide superior adhesion strength. However, in-vivo data suggest that the costs of prolonged adhesion with these materials include instigation of tissue ischemia, inflammation, and undesirable peritoneal adhesion formation [12-15]. Previous studies have even reported high cellular reactivity when fibroblasts are indirectly exposed to cyanoacrylate polymers in an elution test system, as evidenced by suppression of cell proliferation [16].

The state of the art of adhesive sealants for soft tissue applications is summarized in Figure 1 below. *As depicted, an apparent tradeoff exists between the adhesion strength and biocompatibility of currently used materials, limiting the clinical efficacy of adhesive sealants.*
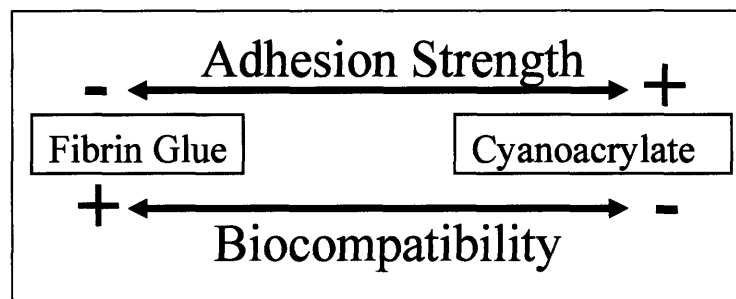
Figure 1: State of the art of adhesive sealants

1.2 Clinical Motivation: Small Bowel Resection

Small bowel resection is a common medical procedure for treating numerous diseases of the gastrointestinal tract [17-19]. Clinical instances of intestinal obstruction or inflammation requiring resection can stem from a variety of conditions, including scar tissue formation, trauma, tissue deformities, gastrointestinal stromal tumors (GIST), and Crohn's Disease [18, 20-23]. Following tissue excision, the created ends of the small intestine are typically reconnected via staples or sutures. Such methodology is generally successful, but post-operative complications are reported in approximately 15% of procedures [24-27]. Risk factors of resection procedures include bleeding, infection, and leakage from the anastomotic site, all which arise primarily from incomplete closure or healing of the surrounding tissue [28-30]. Modification of the anastomotic site to enhance integrity and promote healing is a logical approach to reduce the occurrence of intestinal dehiscence and associated risk factors [9, 11, 31]. Adhesive sealant materials could improve anastomotic healing if used in conjunction with standard closure techniques. *The potential benefits of anastomotic augmentation justify small bowel resection as a physiological model for study of adhesive sealants.*

1.3 Small Bowel Resection: Background and Physiology

1.3.1 The Gastrointestinal Tract

The gastrointestinal (GI) tract provides the body with the central ability to extract nutrients from food and dispense collateral waste. In its totality, the GI tract consists of the mouth, pharynx, esophagus, stomach, small intestine, large intestine, and anus (Figure 2) [32, 33]. As digestion proceeds, food is systematically reduced to small chemical substances and then preferentially absorbed at particular sites throughout the GI cascade. Food processing is obviously essential for health, but is not the only critical function of the GI tract.
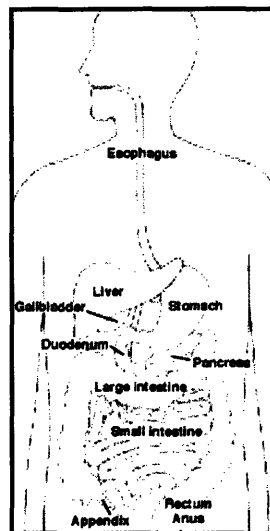
Figure 2: Illustration of the gastrointestinal tract

The immune system is vast and impressive network of defense mechanisms that protect the host from an array of unwanted entities, ranging from particles of sand to viruses. The mouth is a major entry point into the body for foreign substances, implicating the GI tract in immunological defense. Components of the GI tract neutralize invaders with adaptive mechanisms that are in concert with the digestive process. For example, the low acidity of the stomach (pH 1.5-2.0) is maintained by secretion of hydrochloric acid, creating an intolerable environment for many foreign microorganisms and thus facilitating immune defense. Simultaneously, the low pH catalyzes the conversion of pepsinogen to pepsin, a key enzyme in the process of digestion.

The human GI tract is highly developed system of organs with a range of biological functions. Optimal adhesives sealants are expected to differ for each organ of the GI tract due to variations of tissue properties. In this work, the focus is narrowed to the small intestine and methods to improve a standard clinical course followed in disease states, namely small bowel resection.

1.3.2 The Small Intestine

The adult small intestine (intestinum tenue) is an approximately 2.5 cm wide, 7 meter long tubular organ connecting the stomach and the large intestine. About 90% of the absorptive surface area involved in digestion lines the lumen of the small intestine. The majority of nutrient and fat absorption takes place along its length with biochemical reduction of chyme constituents [33]. Absorption occurs via structures termed villi, which are innumerable microscopic extensions of the intestinal wall equipped with lymph capillaries. The small intestine is longitudinally divided into three sections termed the duodenum, jejunum and ileum, as depicted in Figure 3 [34]. The partitioning of the small intestinal is arbitrary to some extent, but some important physiological markers do exist.
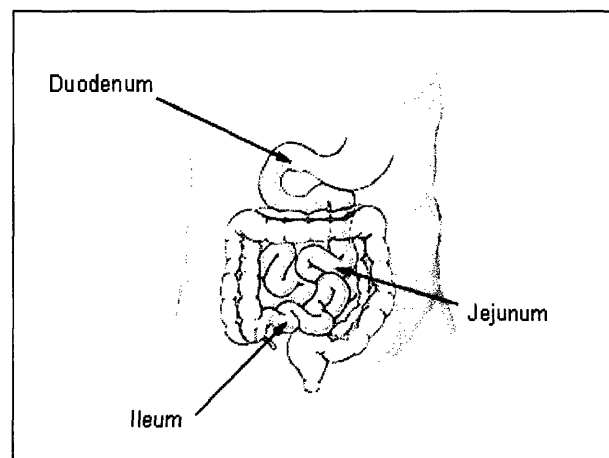
Figure 3: Illustration of the small intestine

Digestion proceeds as food leaves the stomach through the pyloric sphincter and enters the 20-25 cm long, C-shaped duodenum. This section of the small intestine is by far its most

consistent anatomical marker with regards to size and position [35]. In fact, the etymology of duodenum is inspired by its typical '12-finger length' observed amongst patients. Brunner's glands found exclusively in the duodenum secrete alkaline mucus to adjust the pH of incoming acidic gastric chyme and appropriate it for further digestion. The chymeral bolus next enters the less anatomically defined regions of the jejunum and the ileum. One readily detectable difference between these sections is the prominence of mucosal folds appearing in the jejunum as compared to the ileum [36]. These folds, along with the villi structures, have the effect of drastically increasing the absorptive surface area of the small intestine lumen. A gradient of other biological features exists throughout these segments of the small intestine, including entry-to-exit reductions in diameter, wall thickness, vascularity, and depth of color. The small intestine ends with the ileocecal valve, which is the junction between the ileum and large intestine. Digestion continues in the large intestine with the primary purpose of water extraction.

An outward radial description of the small intestinal anatomy begins with the aforementioned villi coverage of the lumen surface. The villi are composed of three main cell types with the following principal functions: epithelial cells for nutrient absorption, enteroendocrine cells for hormone secretion, and globlet cells for secretion of lubricating mucus. The villi and their secretions constitute the mucosal layer of the small intestine. Above the mucosal layer is the thicker muscularis externa, which is further partitioned into an inner circular muscle layer and an outer longitudinal muscle layer. Synchronized contractions of these muscle layers give rise to the mixing of chyme and peristalsis, the active movement of food through the small intestine. The outermost tissue layer for all portions of the small intestine that are not retroperitoneal is the serosa, which is composed of loose connective tissue replete with fibroblasts, smooth muscle cells, fat, and collagen. A mucus secretion covers this external surface and displaces frictional forces generated through inter-organ contact. The small intestine is stabilized within the abdominal cavity by mesenteries connecting it to the abdominal wall [35].

1.3.3 Diseases of the Small Intestine

Disease states of the small intestine can stem from a variety of causes, including neoplastic emergence, anatomical malformations, physical injury and infection. Genetic disposition and lifestyle choices factor in to the occurrence of illness, and can also affect the resulting severity of organ impairment. An exhaustive list of small intestinal diseases and pathological descriptions is not within the scope of this document. Instead, two disease states have been selected to illustrate clinical indications related to the proposed adhesive sealant model application.

Intestinal Obstructions

Intestinal obstructions are marked by partial to complete impedance of food through the intestinal canal, with a documented reoccurrence rate of 33% following diagnosis and treatment [37]. Obstructions can stem from a variety of causes, including scar tissue accumulation or adhesions, paralytic ileus, neoplastic lesions, and infection. Non-surgical or minimally invasive treatment options include stent insertion, enemas, or medication combined with diet modification. In cases of complete obstruction, such as advanced intussusception pictured below [38], more intrusive small bowel resection is the common treatment [39].
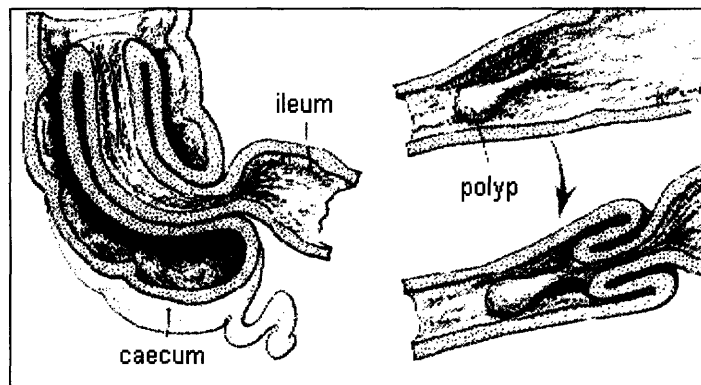
Figure 4: Illustration of intussusception of the small intestine

Crohn's Disease

Crohn's Disease is a chronic inflammatory disease of the GI tract that primarily arises in the ileum of the small intestines. Although Crohn's Disease was first described in 1932 by the physician for whom it is named, the causes remain unknown. In most cases, excessive activation of the immune system leads to ulcerations in the intestinal lining as pictured in Figure 5 [40]. There is no known cure for Crohn's Disease, often leaving surgical treatment as the only viable medical course.
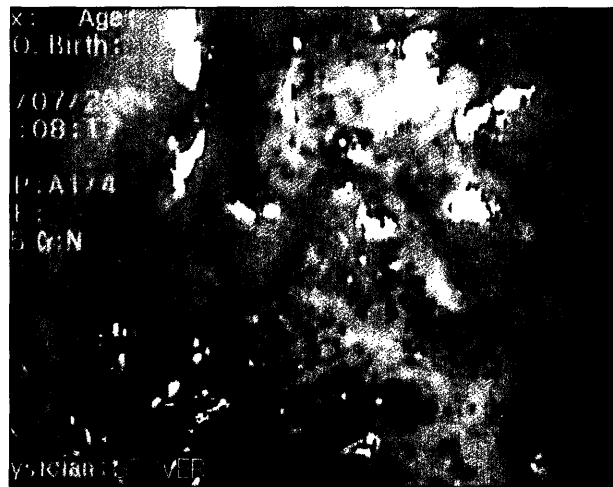
Figure 5: Endoscopic image of ulcer prevalent in Crohn's disease

1.3.4 Small Bowel Resection

As typical of biological designs, organs providing vital functionality are developed in excess. The astonishing length of the small intestine is a prime example of such biological redundancy. It is well established that sufficient digestion can occur with only a fraction of the small intestine in tact. The medical field has taken advantage of this biological feature when presented with the diseased state, and has developed methods for safe removal of ailing tissue. In advanced cases of the disease scenarios described in 1.3.3 and many others, small bowel resection is a clinical course of treatment. Resection procedures consist of surgical removal of a *section* of the small intestine followed by *re*connection of the developed ends at an anastomotic junction. The anastomosis is secured with sutures or staples, usually resulting in a stable junction

requiring no further treatment. However, the available anastomotic techniques are not always effective and occasionally require follow-up surgical procedures.

1.3.5 Risk Factors of Small Bowel Resection

The risks of small bowel resection include those accompanying any procedure requiring general anesthesia, namely medicinal reactions and airway blockage. Risks particular to resection are mainly due to flawed anastomoses. A compromised anastomotic junction can result in intestinal leaks, infection from intestinal bacteria, or excessive bleeding [41]. Resection may lead to a severe reduction in intestinal wall strength, leaving the anastomosis vulnerable to incisional hernia. Peristaltic perturbation of the wound site may result in fatigue failure at the anastomosis.

Depending on the realized severity of these risk factors, a secondary surgical procedure may be necessary [29, 41]. Resection is an invasive procedure and follow-up surgery is highly undesirable. A material augmentation of the suture or staple line may provide a means to reduce the occurrence of anastomotic failure. *A continuous solid material applied to the anastomotic junction could confer two principle advantages; one being a supportive layer to prevent intestinal leakage into the peritoneal space, the other is partial absorbance of forces arising in the sutured or stapled small intestine.*

1.4 Project Overview

Specific material properties of an adhesive sealant have been targeted based on the limitations of small bowel resection procedures. Low viscosity materials allowing administration via injection, controllable in-vivo material swelling and degradation kinetics, biocompatibility, compliance matching to native tissue, bioadhesion, and antibiotic effect could all improve the clinical course following small bowel resection [5, 42, 43].

Hydrogels are a candidate class material that could potentially fulfill these design requirements [44-46]. The biomaterials field has demonstrated that controlling hydrogel properties through network modification is an effective way to meet clinical demands. The high water content and favorable degradation profiles result in good biocompatibility for a wide range of hydrogels. The nature of hydrogel synthesis is also typically amenable to incorporation of bioactive additives, ranging from drugs to cells.

A hydrogel alternative to soft tissue adhesive sealants has been developed by DuPont. The Edelman Lab at MIT, within the framework of the DuPont-MIT Alliance, undertook early and important characterization of the sealant which became the cornerstone for this work [47]. The proposed material is a swellable copolymer consisting of dextran aldehyde and polyethylene glycol (PEG) replete with amine end groups. The two components chemically crosslink through their reactive groups (aldehydes and amines) upon mixing, forming a biodegradable, biocompatible material with adhesive properties, termed a dextran:PEG hydrogel.

Inspired by their potential use as adhesive sealants for soft tissues, the small intestine has been selected as a model organ to study dextran:PEG materials. Key material properties, including hydration and degradation, stiffness, adhesion strength to soft tissue, and biocompatibility, are all expected to greatly influence sealant efficacy upon implantation [11, 48]. Additionally, the available compositional variability for each material component makes a wide range of these properties attainable. Systematic gravimetric, mechanical, and biological characterizations are conducted to understand the relationships between compositional variation and key properties, and to ultimately facilitate application-based compositional design of dextran:PEG materials.

Preliminary experimental results indicate that polymerized dextran:PEG materials are capable of extensive water uptake from an aqueous medium. The materials formed are generally slippery to the touch, clear in color, and flexible. The Schiff base reaction pictured in Figure 6 is reversible, as the network crosslinks are gradually hydrolyzed in aqueous environments.

The composition and processing of the dextran and PEG constituents prior to network formation determine the crosslinked copolymer properties. Specifically, alterations in the solid contents, molecular weights, molecular structure, and available reactive groups will determine the aforementioned material properties desired for adhesive sealant development. *The main focus of this work is understanding the interplay between these compositional variables and key material properties, culminating in the identification of dominant property determinants in dextran:PEG hydrogels.*
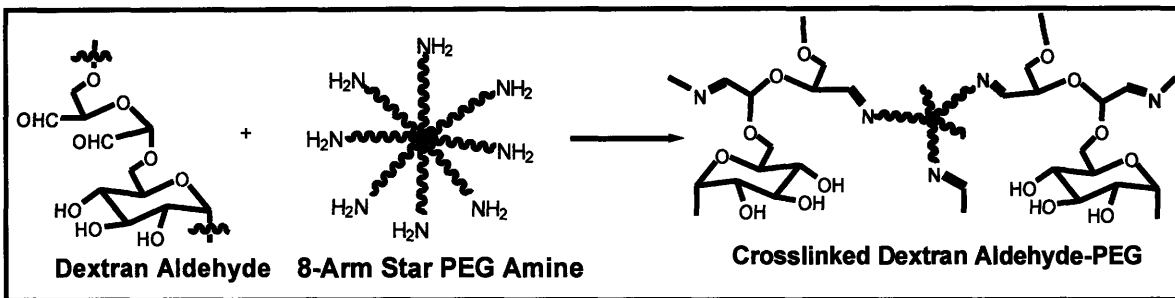
Figure 6: Schematic of dextran aldehyde and PEG amine Schiff base reaction

The limitations of available soft tissue adhesive sealants provide both clinical and scientific motivations for the development of dextran:PEG materials. From a clinical perspective, the need for biocompatible and high strength adhesives is apparent, as available materials suffer from an inverse relationship between these key properties (Figure 1). Scientifically, it is understood that both adhesion strength and biocompatibility depend on chemical reactivity with tissue, and as a result are difficult to independently modify. The compositional complexity of dextran:PEG materials facilitates the development of novel approaches to improving adhesive sealant efficacy, and is the vehicle for studying the effects of compositional variation on key material properties. As diagrammed in Figure 7, the current investigation of dextran:PEG falls within the established paradigm of understanding tissue-material interactions, and could have meaningful impact beyond the progression of soft tissue adhesives.
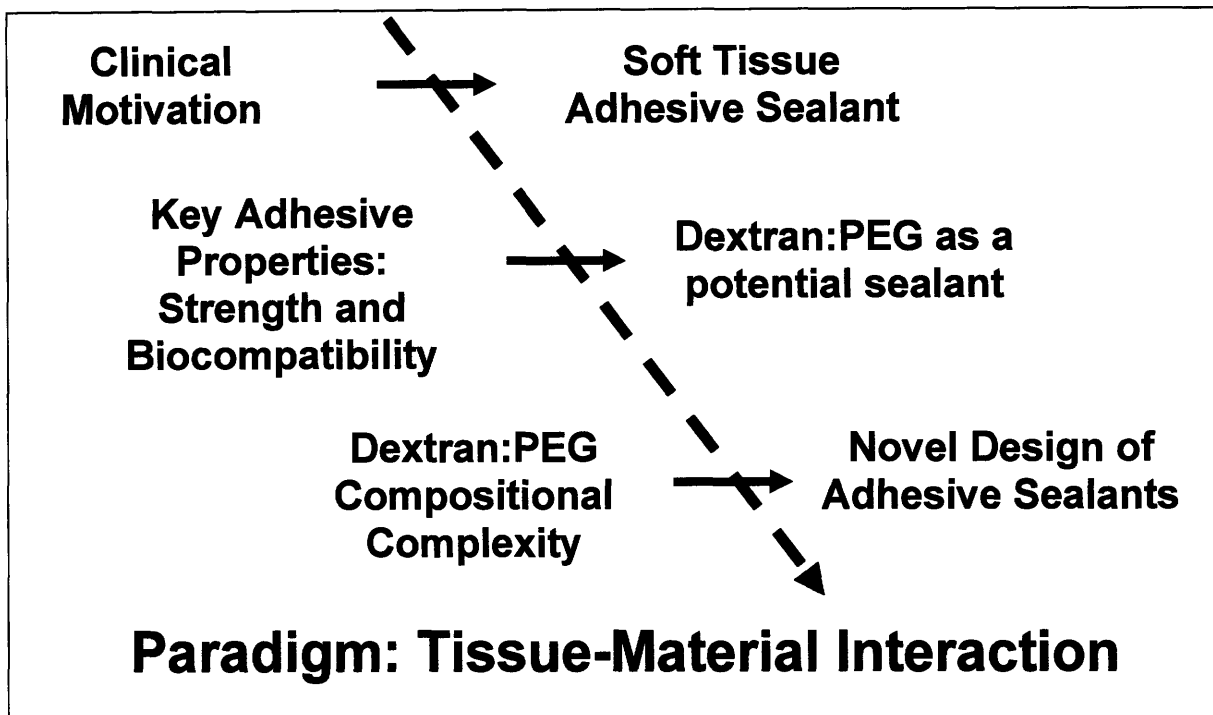
Figure 7: Schematic of dextran:PEG relation to the paradigm of tissue-material interaction

1.5 Nomenclature

The biomaterials studied in this work are copolymers composed of linear dextran aldehydes and polyethylene glycol (PEG) molecules replete with amine end groups. The synthesis of these materials allows for flexibility in a number of compositional variables. The following nomenclature is adopted for the remainder of this work as a means to succinctly denote the composition (a-f) of a particular material formulation.

Dextran aldehyde compositional variables (D)

    a. Molecular weight (kilodaltons)

    b. Oxidative conversion (%)

    c. Solid content (%)

Polyethylene glycol compositional variables (P)

    d. Number of arms per molecule (2 or 8)

    e. Molecular weight of PEG molecule (kilodaltons)

    f. Solid content (%)

The shorthand notation used to quickly identify the composition of these materials reads:

D a-b-c P d-e-f

For example, if a 60 kDa, 20% converted, and 50% solid content dextran aldehyde is combined with an 8-arm, 10 kDa, 60% solid content polyethylene glycol, the resultant copolymer is denoted as:

D 60-20-50 P 8-10-60

1.6 Specific Aims

The main objective of this work is to identify key property determinants of dextran:PEG materials with respect to compositional variations. A secondary objective is to collectively analyze these property data to propose an optimal material formulation for a small bowel resection adhesive sealant model. Eventually, extension of identified property determinants into other material systems will be explored as a means to propagate sealant technologies. The following specific aims outline a path to realizing these objectives.

1. Rate the hydration and degradation properties of various dextran:PEG material formulations.

2. Quantify material stiffness and adhesion strength to soft tissue for various dextran:PEG formulations.

3. Analyze the effect of compositional variation on key material properties. Identify property determinants with respect to material compositional variables.

4. Quantify the proliferative and cytotoxic effects of dextran:PEG materials. Identify the cellular response to variation of material composition.

5. Merge gravimetric, mechanical and biological data to propose an optimal dextran:PEG material formulation for a model adhesive sealant application.

1.7 Summary of Findings

Intermittent gravimetric analyses of dextran:PEG suspensions in aqueous media were used to assess material hydration and degradation properties (Specific Aim 1). Uniaxial tensile testing and tissue-material interface displacements were used to effectively quantify dextran:PEG elastic moduli and the adhesion strengths to excised tissue, respectively (Specific Aim 2). Main effect analyses and multiple linear regressions were used to model the effect of compositional variation on these material properties and identify the most influential compositional variables. Three dominant property determinants were identified in dextran:PEG materials: network complexity (PEG arm number) determines material hydration and catastrophic degradation time, PEG solid content determines elastic modulus, and the available aldehyde groups determines adhesion strength to tissue (Specific Aim 3).

In-vitro studies utilizing mammalian cell cultures provide preliminary indication of dextran:PEG biocompatibility. The conducted studies investigate the influence of material solid content (dextran solid content + PEG solid content) and reactive group ratio (aldehyde:amine) on cell reactivity. Cytotoxicity studies reveal that degradation by-products from dextran:PEG suspensions generally have a mild cytotoxic effect on cell cultures. Furthermore, the cytotoxic effect is eliminated in materials with intermediate levels of reactive group ratio and solid content. Proliferation assays were conducted to explore the effects of direct dextran:PEG applications to cell cultures. The cellular responses to dextran:PEG formulations ranged from inhibition to stimulation of proliferation, with a positive dependence on material aldehyde content. Similarly to cytotoxicity studies, a material formulation with intermediate reactive group ratio had no effect on cell proliferation (Specific Aim 4).

The collection of data regarding dextran:PEG materials (Specific Aims 1-4) were processed to yield an optimized compositional formulation for a model adhesive sealant application (Specific Aim 5). The property selection criteria for dextran:PEG materials include high swelling ratio, long degradation times, compliance-matching to tissue, and minimal reactivity with cells. The following dextran:PEG composition is predicted as optimal for anastomotic augmentation: D 48-24-50 P 8-4-20. Future experimentation with dextran:PEG materials will seek correlations between in-vitro property data and in-vivo material performance.

Chapter 2: Theory

Chapter 2 begins with justification of focus on particular material properties for study of adhesive sealants (Section 2.1). Dextran:PEG material constituents and the expected effects of compositional variation on material properties are then summarized (Section 2.2). Chapter 2 concludes with an overview of the optimization procedure utilized for application-based dextran:PEG compositional design (Section 2.3).

2.1 Important Material Properties of Adhesive Sealants

Hydration and Degradation

The in-vivo hydration and degradation properties of an adhesive sealant will determine the constitutional similarity of the material to adhered tissue and the duration of material function, respectively. Because soft tissues are highly hydrated materials, superabsorbent sealants should have good biocompatibility as they approximate tissue composition [45]. Dextran:PEG hydrogels consist of hydrophilic polymer networks, potentially providing the desired material mimicry of soft tissue hydration. However, the high water content of these materials makes network crosslinks increasingly susceptible to hydrolytic breakdown.

By definition, highly swollen materials incorporate more water into their free volume as compared to less absorbent alternatives. The surplus of water within an extensively hydrated material will generally accelerate the hydrolytic breakdown of network crosslinks, resulting in bulk material degradation [49]. Following significant degradation, adhesive sealants can no longer meet functional requirements, including adherence to tissue, prevention of leaks, and absorbance of mechanical loads. The aldehyde-amine crosslinks formed in dextran:PEG are susceptible to hydrolytic degradation, although bond exposure to hydrolytic activity can potentially be reduced through complex network formation. A clinically effective dextran:PEG sealant would ideally undergo extensive swelling prior to the onset of bulk degradation.

Material Stiffness

A tissue-material mechanical compliance mismatch can potentially reduce the clinical efficacy of medical products designed for soft tissue applications. Small diameter (less than 5

mm internal diameter) synthetic vascular grafts are an example of a medical product limited by compliance mismatch to tissue. Failed attempts at graft development are frequently attributed to lumen restenosis from vascular smooth muscle cell hyperplasia, with the cellular response seemingly accelerated at compliance-mismatched anastomoses [50, 51].

Compliance mismatch between adhered tissue and sealant materials is also a limitation of soft tissue adhesives. Overly stiff materials, such as cyanoacrylates, lack necessary flexibility to deform with soft tissues under load, potentially resulting in stress concentrations and tearing in the tissue. Fibrin glues have a mechanical compliance more similar to tissues, but are not optimal sealants due to high in-vivo degradation rates and low adhesion strengths. A compliance-matched yet highly adhesive material could improve the efficacy of soft tissue sealants.

Adhesion Strength to Soft Tissue

Bioadhesive strength is the primary functional property for adhesive sealant materials. Sealants with sufficient adhesion strength will remain attached to tissue throughout the desired implant lifetime, thus providing the expected clinical benefit. The required sealant adhesive strength for a given application is dictated by the loads transferred to the tissue-material interface in-situ. In the case of small bowel anastomotic reinforcement with adhesive materials, a cyclical pressure wave with approximate 10 min^{-1} frequency and 30 mmHg amplitude will be partially transmitted to the applied sealant through the intestinal wall [52]. Adhesion strength is fundamentally dependent on the reactivity of a material with tissue, necessitating tissue-specific characterization of this property for effective sealant design.

Biocompatibility

Acceptable biocompatibility of any material must be established prior to clinical use. The inverse relationship between biocompatibility and adhesion strength depicted in Figure 1 limits the efficacy of currently available sealants [53]. Similar to adhesion strength, biocompatibility is dependent on the extent and nature of chemical reactions between the tissue and material. The common dependence of multiple sealant properties (adhesive strength and biocompatibility) on tissue-material reactivity demands multiple characterizations for adhesive development.

2.2 Dextran:PEG Constituents and Compositional Variation

The following section describes the two components of dextran:PEG copolymers (Section 2.2.1) and the expected effects of compositional variation on material properties (Section 2.2.2).

2.2.1 Constituents of Dextran:PEG Materials

Dextran Aldehyde

Dextran is a polysaccharide of glucose molecules joined via glycosidic linkages. Linear dextrans of various molecular weights are oxidized with sodium periodate, yielding dextran aldehyde with reactive groups forming throughout the entire length of the molecules (Figure 8). The extent of oxidation is determined by the initial molecular weight of the dextran molecules and the relative amount of sodium periodate with which it is reacted. A calculable number of aldehyde groups will be available for network formation when polymerized with the aminated PEG component. Aldehyde groups which remain unreacted following network formation will potentially facilitate bioadhesion, as previous studies have indicated that oxidized dextran readily reacts with tissues [54, 55].

Dextran   **Dextran aldehyde**
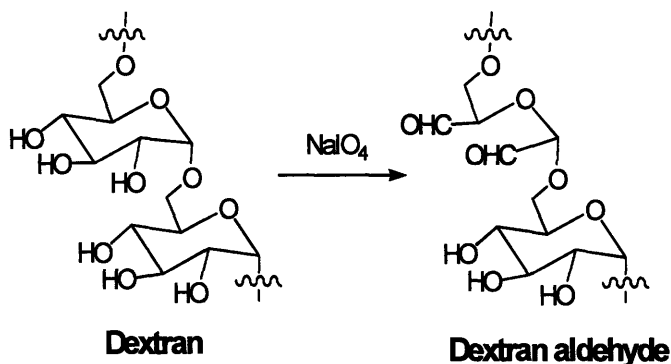
Figure 8: Oxidation of dextran to yield dextran aldehyde

Aminated Polyethylene Glycol

PEG with amine end groups is prepared in two forms: linear and star-shaped molecules. The linear PEG has two amine groups per molecule, while the star PEG consists of eight PEG chains joined at the center of a complex macromolecule, and thus carries eight amine groups per molecule (Figure 9). Dextran:PEG polymerization is spontaneous upon component mixing at room temperature, as the PEG amine groups readily react with the aldehyde groups of the dextrans. Amine reactivity with tissue could also potentially contribute to copolymer bioadhesion.
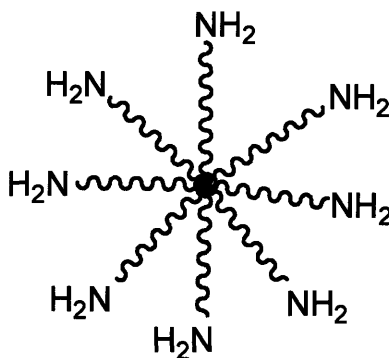
Figure 9: Schematic of aminated star PEG molecule

Dextran:PEG Polymerization

The dextran and PEG components are separately prepared as aqueous solutions with low viscosities. The highest solid content formulated for either component (60 w.t.%) has low enough viscosity to allow for easy injection through a 5 ml syringe and a 20-gauge needle at room temperature. Prior to polymerization, equal volumes of material components are loaded into separate chambers of a dual chamber syringe. A 12-step mixing tip is attached to the syringe (Figure 10) as a means to promote repeatable and extensive mixing of the two components. Following mixed injection, the dextran aldehyde and aminated PEG form a chemically crosslinked copolymer network within seconds, as diagramed in Figure 6.
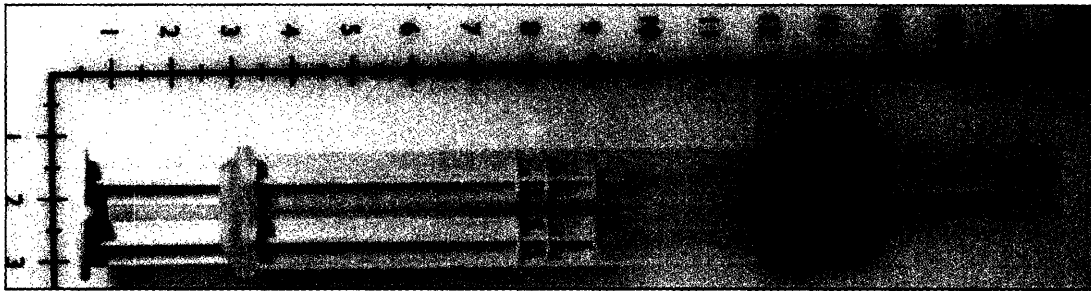
Figure 10: Dual chamber syringe with mixing tip used for dextran:PEG polymerization

2.2.2 Expected Effects of Compositional Variations in Dextran:PEG

Dextran Molecular Weight (D_MW, units kDa)

A complex crosslinked network forms following polymerization of PEG and dextran molecules. Due to the complexity of the developed network (especially with use of star PEG molecules), steric effects could potentially hinder crosslinking between component reactive groups (aldehydes and amines). Comparison of the molecular weight ranges of each material component (PEG: 2 – 10 kDa, dextran: 10 – 60 kDa) suggests that molecular dimensions of larger dextran molecules (60 kDa) may sterically hinder bond formation to a greater extent than those closer in size to the PEG (10 kDa), ultimately yielding less stiff networks. Additionally, increasing dextran length likely increases the average molecular weight between network crosslinks, which is predicted to reduce stiffness in the standard theory of rubber elasticity [48]. These two factors suggest that dextran molecular weight in dextran:PEG materials will negatively correlate with elastic modulus.

Adhesive strengths of dextran:PEG copolymers are dependent on surface reactivity at material-tissue interfaces. Increasing the molecular weight and correspondingly the flexibility of the constituent dextran aldehyde could provide a physical means to encourage chemical bonding at an interface. The adhesive strengths of dextran:PEG are expected to positively correlate with molecular weight by virtue of increased interaction with juxtaposed tissue [56].

The positive relationship intuited above between dextran aldehyde molecular weight and adhesive strength directly contradicts an established fact: the most biologically reactive aldehyde, formaldehyde, is also the smallest aldehyde. The diminished reactivity seen in intermediate sized aldehydes as compared to formaldehyde, such as gluteraldehyde, is due to a reduction of molecular mobility. The relatively low molecular mobility limits penetration depth into tissue and prevents complete chemical reaction. It is hypothesized that in aldehyde-based adhesive sealants, where functional chemical bonds link the tissue to the polymer network, the diminished reactivity of large aldehydes can be recovered when molecular chains exceed a critical length, due to compensation of mobility-induced hindrance by increased molecular flexibility at the material-tissue interface. It is further hypothesized that as dextran:PEG copolymers degrade, larger constituent dextrans will induce relatively little cytotoxicity in surrounding tissues, by virtue of their limited mobility and penetration depth into tissue.

Dextran Oxidative Conversion (D_OX, units %)

Oxidative conversion of hydroxyl groups imparts reactive aldehydes to surface-present dextran (as well as bulk dextran), and is expected to positively correlate with adhesion strengths in dextran:PEG materials. The effect of oxidative conversion on elastic modulus is expected to be positive to the extent to which additional crosslinks are formed due to elevated reactive group availability. Once aldehydes are present in excess in the crosslinked material, there will be no additional increase in elastic modulus as oxidation is increased.

As dextran:PEG materials undergo degradation, the number of free aldehyde groups available for cytotoxic interactions with tissue depends on initial dextran oxidation. Free aldehydes can have high reactivity with cells, as evidenced by the use of formaldehyde as a common tissue fixative. Due to increased reactivity, a positive correlation is expected between dextran oxidative conversion (specifically the resultant material aldehyde content) and cellular reactivity when cells are exposed to various dextran:PEG materials.

Dextran Solid Content (D_SC, units %)

Increasing the weight percent of solid dextran in dextran:PEG is expected to positively correlate with adhesion strength and elastic modulus [57]. The increased solid content will increase the stiffness of the material via network crosslinking and chain immobilization, as well as the number of aldehyde reactive groups available for adhesion to tissue.

Similar to dextran oxidative conversion, increasing dextran solid content increases the number of free aldehyde groups produced upon dextran:PEG network degradation. However, the degradation rate of high solid content materials will be relatively slow, resulting in a gradual release of reactive degradation products. Consequently, a negative correlation is expected between dextran solid content and the degradation-induced cytotoxicity due to a relatively prolonged hydrolytic breakdown of highly polymerized (high solid content) materials. However, a positive correlation between cell reactivity and solid content is expected when materials are applied in bulk form or when degradation products are pooled over time, as the higher solid content dextran:PEG will present more aldehyde groups for interaction with cells in these scenarios.

Number of arms per PEG molecule (P_ARM, units number [2 or 8])

As the number of arms per PEG molecule is increased in dextran:PEG, there is a corresponding increase in resultant network complexity and a reduction in polymer chain mobility. The increased network complexity of star PEG-containing material formulations (as compared to linear PEG) is expected to shield the copolymer network from hydrolytic degradation, resulting in relatively protracted degradation kinetics.

Polymers are typically capable of undergoing large strains prior to failure due to individual chains unfolding, stretching and sliding to accommodate loads. In complex copolymer networks with limited molecular mobility, a more brittle-like failure response is possible. A transition from a traditional ductile to a more brittle mechanical response to load is anticipated as the number of PEG arms is increased in dextran:PEG materials.

PEG Molecular Weight (P_MW, units kilodalton)

As with dextran molecular weight, the expected effect of PEG molecular weight variation on elastic modulus is influenced by the possibility of steric hindrance of network formation and the standard theory of rubber elasticity. In this case, due to the generally diminutive size of the PEG molecules in comparison to the dextrans (PEG: 2 – 10 kDa, dextran: 10 – 60 kDa), it is expected that steric effects would be more restrictive in networks comprised of the smallest PEG molecules. However, smaller PEG molecules should yield stiffer copolymer networks in regards to the molecular weight-modulus relationship posited by the standard rubber elastic theory. These opposing hypotheses make it difficult to predict the net effect of PEG molecular weight variation on elastic modulus, and suggest that experimental investigation of this compositional variable is crucial for material design. In terms of adhesion to soft tissues, it is again expected that larger molecules will facilitate more interaction with tissue surfaces, and thus provide greater adhesion strengths [56].

PEG Solid Content (P_SC, units %)

Similarly to the expected effect of dextran solid content, PEG solid content will likely positively correlate with material modulus. An increase of material content will increase the microscopic network density and in turn the macroscopic elastic modulus. The adhesion strength is expected to have no correlation or a positive correlation to PEG solid content, depending on the extent of amine reactivity with tissue.

The same rationale put forth for dextran solid content applies to the expected biological effect of PEG solid content; the cellular response to dextran:PEG materials with varying PEG solid content will depend on the mode of cellular exposure to a material and the developed degradation products. If degradation products are pooled or the material is presented in the bulk form, a positive correlation between PEG solid content and cellular reactivity is expected. If the degradation products of dextran:PEG are gradually cleared away from a the cellular environment (as typically occurs in-vivo), a negative dependence of cell reactivity on PEG solid content is expected, as the slower degrading (high solid content) materials will result in lower transient concentrations of potentially reactive by-products.

Table 1 summarizes the expected effects of compositional variation on selected dextran:PEG properties. The "+" and "-" symbols indicate that a positive or negative correlation is expected between the tabulated compositional variable and material property, while a "?" indicates differing expectations on the expected nature of the variable-property relationship.

Table 1: Summary of expected effects of compositional variation on dextran:PEG properties

Compositional Variable	Elastic Modulus	Adhesion Strength	Biocompatibility
Dextran mw	-	+	+
Dextran solid content	+	+	-
Dextran oxidation	+	+	-
PEG mw	?	?	?
PEG solid content	+	-	+
PEG arm number	+	?	?

2.3 Property Determinants and Compositional Optimization

Key material properties for adhesive sealants include swelling ratio, degradation rate, compliance, adhesion strength, and biocompatibility (Section 2.1). The range of available variation of dextran:PEG compositions facilitates optimization between these key properties, providing a means for application-based design of material formulations. The experimental data generated in this work are sufficient for a preliminary optimization between compositional variables with respect to targeted material properties. More refined optimization would require development of material property characteristic curves, which in turn requires analyses of prohibitively large design spaces (six independent compositional variables).

The strategy followed for preliminary optimization of dextran:PEG as a potential adhesive includes analyses of mechanical properties (stiffness and adhesive strength) at extremes of isolated compositional variation. For example, to quantify the effect of dextran molecular weight on material stiffness, uniaxial tensile tests are conducted on pairs of materials that differ only in this compositional variable. In each pair, the constituent dextran molecular weight of one material is the low end of available variation (10 kDa), while the other is the high end (60 kDa). Comparing the property response to isolated variations in multiple material pairs provides coarse indication of the main effect of dextran molecular weight on dextran:PEG polymer stiffness. Main effect analyses appreciably reduce the size of the experimental design space needed to identify basic data trends, but of course are limited by the associated simplifications assumed for the material property response. As with most optimization problems, a decision regarding the appropriate level of material characterization is implicit in the design process. The limitations and utility of the material property data are further discussed in Section 5.

The gravimetric (swelling and degradation) and biocompatibility (cytotoxicity and proliferation) studies conducted with dextran:PEG materials consist of more traditional design spaces. In these cases, the tested material formulations are more continuous with regards to a targeted compositional variable. For example, the expected importance of network reactive groups on dextran:PEG reactivity with cells motivates cytotoxic analysis at multiple levels of reactive group ratio.

A goal of this work is to collectively use the generated data to select a candidate material for future dextran:PEG in-vivo studies. Material property data inform the optimization of composition by providing either bounds on a particular variable or a means to target a specific material property value, as described in Section 4.5.

Chapter 3: Experimental Methods

The following chapter describes the experimental methods for gravimetric, mechanical and in-vitro biological testing of dextran:PEG hydrogels. Gravimetric analyses of aqueous dextran:PEG suspensions were used to calculate material swelling ratios and catastrophic degradation times (Section 3.1). Uniaxial tensile testing was used to determine the elastic moduli of selected material formulations (Section 3.2). Controlled interface displacements were used for quantification of dextran:PEG adhesion strengths to excised tissue (Section 3.3).

The cellular response to dextran:PEG copolymers was analyzed with cytotoxicity and proliferation assays. Smooth muscle cells were exposed to pooled degradation supernatant from dextran:PEG suspensions to determine the effect of material composition on by-product cytotoxicity. Fibroblast proliferation assays were conducted following direct application of dextran:PEG to fibroblast cultures, providing preliminary indication of polymerized material biocompatibility (Section 3.4).

3.1 Gravimetric Analysis

Hypotheses

Hydration and degradation properties in copolymers can be simultaneously improved with the use of complex hydrophilic network constituents with propensity for chain entanglement. The inclusion of star PEG in dextran:PEG copolymers will significantly increase the crosslinked network complexity as compared to linear PEG, resulting in increased swelling ratio and persistence time prior to catastrophic degradation in an aqueous suspension.

Experimental objectives

Analyze the hydration and degradation properties of dextran:PEG materials with a gravimetric method. Based on gravimetric data of swollen material samples, calculate dextran:PEG swelling ratios and times until onset of catastrophic degradation. The swelling ratio of dextran:PEG samples is calculated as follows,

$$\text{Swelling Ratio}(\%) = \left[\frac{W_\infty - W_D}{W_D}\right] \times 100$$

where W_∞ is the maximal disk mass measured throughout the suspension period and W_D is the initial disk mass prior to suspension (dry sample). The onset of catastrophic degradation is defined as the time after initial suspension in an aqueous medium at which the material sample begins to lose net mass.

Use multiple linear regressions to model the relationships between compositional variables (inputs) and the gravimetric data (outputs). Compute the correlations between the gravimetric data and dextran:PEG compositional variables.

Experimental procedure

The following procedure was used to assess hydration and degradation properties of dextran:PEG materials:

1. Prepare dual chamber syringes with dextran aldehyde and aminated PEG components described in Table 2.
2. Polymerize dextran:PEG materials in disk-shaped molds (8 mm diameter, 3 mm thick). Prepare samples in triplicate.
3. Extract dextran:PEG samples from molds. Measure sample diameters with digital calipers.
4. Weigh samples prior to hydration with a digital scale.
5. Prepare an aqueous suspension of each sample (100 ml MilliQ Water, 250 ml glass beaker).
6. Weigh and measure sample dimensions at predetermined time points.
7. Record and analyze gravimetric data with Excel and Minitab softwares.

Table 2: Dextran:PEG samples prepared for gravimetric analyses

Sample Label	CHO:NH$_2$
D 10-50-7 P 2-2-50	0.96
D 60-20-25 P 2-2-30	2.14
D 10-50-20 P 2-2-50	2.74
D 10-50-25 P 2-2-50	3.42
D 10-50-45 P 2-2-30	10.27
D 10-50-5 P 8-10-40	1.07
D 10-50-5 P 8-10-38	1.13
D 60-20-15 P 8-10-38	1.27
D 10-50-14 P 8-10-40	3.00
D 40-25-15 P 8-10-20	3.04
D 60-20-20 P 8-10-21	3.06
D 10-50-14 P 8-10-21	5.71
D 40-25-25 P 8-10-10	10.15
D 10-50-25 P 8-10-21	10.19

3.2 Uniaxial Tensile Testing

Hypotheses

The elastic modulus of copolymers with constituents featuring varying degrees of complexity (linear versus star molecules) is primarily determined by the percent solid content of the more complex molecular component. In the case of copolymers featuring star PEG and linear dextran, star PEG solid content will have the strongest positive correlation to material stiffness.

Experimental objectives

Measure the elastic moduli of selected dextran:PEG materials via uniaxial tensile testing. Identify the primary compositional determinants of dextran:PEG elastic modulus. Quantify the material stiffness response to compositional variation with a multiple linear regression model.

* Based on the data from the gravimetric studies (Section 4.1), present and subsequent experiments (Sections 3.2-3.4) are limited to dextran:PEG formulations featuring constituent star PEG (as opposed to linear PEG).

Experimental procedure

Moderate uniaxial displacements (stretch ratio < 1.15) are used to capture the linear regime of elastic deformation in dextran:PEG hydrogels. An ElectroForce® 3450 mechanical tester (22 N load cell and up to 5 mm displacement stroke) is used for uniaxial tensile. Uniform testing regions of cast dog bone-shaped material specimens (Figure 11) are extended at constant displacement rate of 0.05 mm per second with the Electroforce® system. The force required to maintain the displacement rate is recorded by the system load cell. Force versus displacement data is then transformed to true stress versus stretch ratio plots for each sample. The elastic modulus of each dextran:PEG sample is the slope of the generated true stress versus stretch ratio plot [58].

The dog bone-shaped samples of dextran:PEG materials produced for uniaxial tensile testing do not conform to ASTM standards. The samples used are thicker in the middle region than prescribed by ASTM. Efforts made to cast samples within the geometrical guidelines were thwarted by an inability to remove polymerized specimens from the molds without inducing

damage. Even when specimens were extracted from molds in the hydrated state to reduce friability, tears at the material-mold interface would ruin the samples. Nevertheless, the utilized dog bone-shaped geometry was sufficient to yield repeatable measurements of material elastic moduli and prevent tearing at the sample-grip interface.
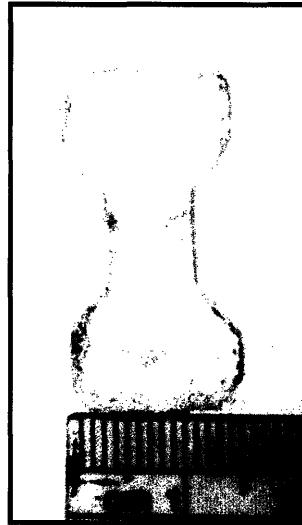
Figure 11: Dextran:PEG dog bone-shaped sample for uniaxial tensile testing

The dextran:PEG design space (Table 3) chosen for uniaxial tensile testing facilitates comparison of material moduli at low and high compositional variable levels in otherwise identical material pairs. Three such low versus high comparisons of elastic moduli are made for each compositional variable. Figure 12 schematically depicts the *main effect* calculation of constituent dextran molecular weight on dextran:PEG modulus; main effects are similarly determined for each compositional variable. As seen in Figure 12, the average change in elastic moduli measured between the three low and high pairs for a given compositional variable is the calculated variable main effect. The relative magnitudes of the variable main effects are used to discern the compositional determinants of material properties. The benefits and limitations of the main effect analyses are discussed in Section 5.1.

Table 3: Dextran:PEG samples prepared for uniaxial tensile testing

Sample Label	CHO:NH₂
D 10-20-20 P 8-2-20	0.64
D 60-20-20 P 8-2-20	0.64
D 10-20-20 P 8-10-60	1.07
D 60-20-20 P 8-10-60	1.07
D 10-20-40 P 8-2-20	1.29
D 10-50-20 P 8-2-20	1.71
D 10-20-40 P 8-10-60	2.14
D 10-50-20 P 8-10-60	2.85
D 10-20-20 P 8-10-20	3.21
D 60-20-20 P 8-10-20	3.21
D 10-20-40 P 8-10-20	6.43
D 10-50-20 P 8-10-20	8.56

Dextran Molecular Weight Main Effect

	Variable Low		Variable High
i=1	D 10-20-20 P-8-2-20	vs	D 60-20-20 P-8-2-20
i=2	D 10-20-20 P-8-10-60	vs	D 60-20-20 P-8-10-60
i=3	D 10-20-20 P-8-10-20	vs	D 60-20-20 P-8-10-20

Dextran Solid Content Main Effect

Dextran Oxidation Main Effect

PEG Molecular Weight Main Effect

PEG Solid Content Main Effect

Main effect of Dextran Molecular Weight on Dextran:PEG Modulus
The average change in dextran:PEG modulus for the three isolated low-to-high variations of constituent dextran molecular weight

$$\text{Main Effect} = \frac{\left[\sum_{i=1}^{3} \frac{(\text{High Varible Modulus})_i - (\text{Low Variable Modulus})_i}{(\text{Low Variable Modulus})} \right] \times 100}{3}$$
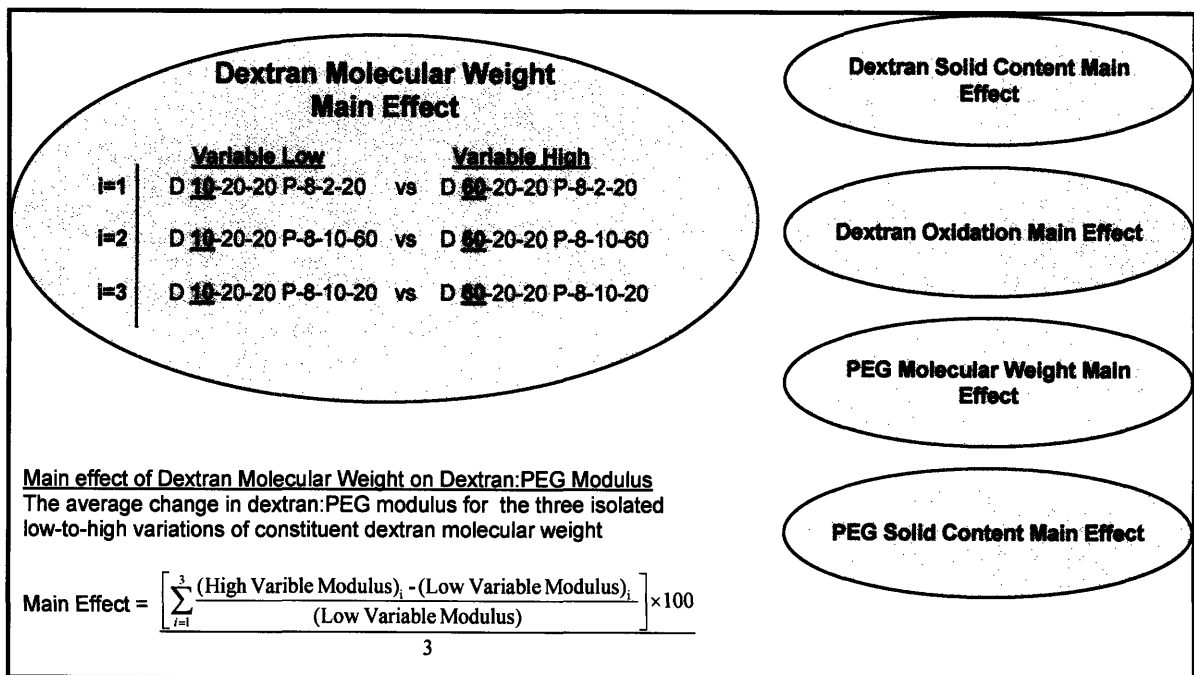
Figure 12: Schematic of main effect analyses of dextran:PEG moduli

The following procedure is used to measure the elastic moduli of dextran:PEG materials:

1. Prepare dual chamber syringe with specific dextran aldehyde and aminated PEG (Table 3).

2. Polymerize materials with a dual chamber syringe and a 12-step mixing tip into dog bone molds, with extension region dimensions of: length = 10 mm, width = 8 mm, and thickness = 6 mm.

3. Flatten top and bottom of sample with glass cover slips.

4. Allow sample to cure for 1 minute. Gently remove cover slips.

5. While sample is in the mold, add 1 ml of 1X phosphate buffered saline (PBS) to top side. Allow PBS to absorb for 30 seconds.

6. Repeat step 5 with sample bottom side.

7. Carefully remove sample from mold.

8. Repeat steps 5 and 6 with sample out of mold.

9. Apply a displacement rate-controlled uniaxial extension to the sample with Electroforce® mechanical tester and the following parameters:
    a. Ramp displacement profile (monotonically increasing, constant rate)
    b. 1.2 mm total displacement
    c. Displacement rate of 0.05 mm/sec

10. Capture force/displacement data throughout entire 1.2 mm extension.

11. Transfer data to Excel file.

12. Record and analyze uniaxial tensile data with Excel and Minitab softwares.

3.3 Adhesion Strength Testing

Hypotheses

Dextran:PEG copolymers will adhere to soft tissue based on the available material reactive groups localized to the tissue-material interface. Materials featuring excessive aldehyde reactive groups will have enhanced adhesive capability, due to chemical bonding with amine groups of cell surface proteins. The bioadhesive strengths of dextran:PEG copolymers will be primarily determined by the concentration of aldehyde groups at the tissue-material interface.

Experimental objectives

Determine the adhesion strength of dextran:PEG materials to excised intestinal tissue. Identify the primary compositional determinants of dextran:PEG adhesive strength. Quantify the adhesive strength response to compositional variation with a multiple linear regression model.

Experimental procedures

The bioadhesive strength of dextran:PEG to the serosal surface of rat small intestine is measured through application of a tensile force to a tissue-material-tissue interface (Figure 13). As with uniaxial tensile testing, the material design space for adhesion strength testing facilitates estimation of compositional variable main effects on the property of interest (Table 4). Two serosal surfaces are joined with a dextran:PEG polymer, with subsequent application of a tensile force. The maximal force detected prior to interface failure reflects the bioadhesive strength of the material formulation used to join the tissue samples.

Upper Mechanical Testing Grip

Polymerize PEG:Dextran Form Tissue-Material-Tissue Interface

Excised Tissue Samples (Threaded w/ Si Tube)

Lower Mechanical Testing Grip
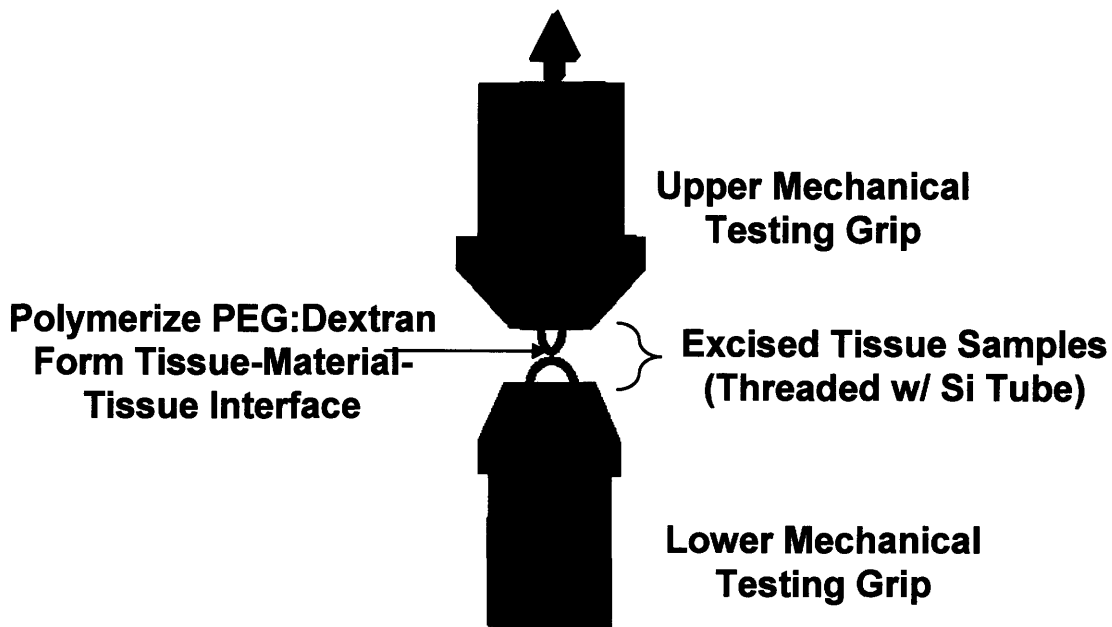
Figure 13: Schematic of adhesion strength testing procedure

Table 4: Dextran:PEG samples prepared for adhesion strength testing

Sample Label	Stress (kPa)
D 10-20-20 P 8-2-20	0.64
D 60-20-20 P 8-2-20	0.64
D 10-20-20 P 8-10-60	1.07
D 60-20-20 P 8-10-60	1.07
D 10-20-40 P 8-2-20	1.29
D 10-50-20 P 8-2-20	1.71
D 10-20-40 P 8-10-60	2.14
D 10-50-20 P 8-10-60	2.85
D 10-20-20 P 8-10-20	3.21
D 60-20-20 P 8-10-20	3.21
D 10-20-40 P 8-10-20	6.43
D 10-50-20 P 8-10-20	8.56

The following procedure is used to measure the adhesion strengths of dextran:PEG materials to excised intestinal tissue:

1. Prepare dual chamber syringe with specific dextran aldehyde and PEG materials (Table 4).

2. Anesthetize two rats (Sprague-Dawley, female, 258 g and 277 g) with standard ketamine and xylazine cocktail.

3. Sacrifice rats using carbon dioxide asphyxiation.

4. Directly following sacrifice, harvest small intestine. Remove all waste products from intestinal lumen.

5. Store harvested tissue in Krebs-Henseleit buffer at room temperature throughout duration of experiment (10 hours).

6. Cut 25 mm longitudinal sections of small intestine.

7. Thread two small intestine sections with silicon tubes (2.4 mm o.d., 25 mm length).

8. Bend silicon tubes with threaded intestines, bringing sample ends together.

9. Secure one sample (in bent configuration) in each vice grip of mechanical tester. The bent configuration promotes sample stability throughout mechanical test (Figure 14).

10. Using dual chamber syringe, polymerize 0.25 ml total volume of a test material onto bottom intestinal sample.

11. Immediately bring samples together such that intestinal samples are in contact through the material, and a zero or near zero load is detected by the load cell. Allow 1 minute for material to cure and achieve adherence with tissue surfaces.

12. Apply a constant rate displacement of 0.05 mm/sec over 4 mm total displacement.

13. Capture force/displacement data.

14. Record and analyze adhesion strength data with Excel and Minitab softwares.

3.4 Cytotoxicity and Proliferation Testing

Cytotoxicity (Section 3.4.1) and proliferation (Section 3.4.2) assays were conducted to determine the effects of dextran:PEG bulk copolymers and degradation products on cell cultures. The in-vitro data provides preliminary indication of material biocompatibility and direction for dextran:PEG compositional design.

3.4.1 Cytotoxic Effect of Dextran:PEG Degradation Products

Hypotheses

The cytotoxic effects of copolymer degradation products will be greater for material formulations featuring an excess of aldehyde groups ($CHO:NH_2 > 1$). If material degradation products are pooled following long degradation times (such that materials have completely dissolved), degradation-induced cytotoxicity will positively correlate to material solid content.

Experimental objectives

Determine the cytotoxic effect when smooth muscle cell cultures are exposed to dextran:PEG degradation products. Rate the effect of material reactive group ratio and solid content on degradation-induced cytotoxicity.

Experimental procedure

The response of vascular smooth muscle cells (vSMC, bovine source) to pooled dextran:PEG degradation products is quantified with cytotoxicity assays. Comparisons are made between the degradation products of materials with various total solid contents and reactive group ratios. The selected materials allow for comparison of both material solid content and reactive group ratio at four levels (Table 5). The first four tabulated samples span a range of wide solid contents (12.5 %– 42.5 %) with limited variance in reactive group ratio (2.11-2.96), while the second four samples span a wide range of reactive group ratios (0.42-10.7) with limited variance in solid content (21.5 %-22.5%). The effect of material degradation products on vSMC provided preliminary indication of dextran:PEG biocompatibility [59].

Table 5: Dextran:PEG samples prepared for cytotoxicity testing

Sample Label	Total Solid Content (%)	CHO:NH$_2$
D 10-50-5 P 8-10-20	12.5	2.14
D 60-20-25 P 8-10-38	31.5	2.11
D 60-20-35 P 8-10-38	36.5	2.96
D 60-20-35 P 8-10-50	42.5	2.25
D 60-20-5 P 8-10-38	21.5	0.42
D 10-50-5 P 8-10-38	21.5	1.13
D 60-20-25 P 8-10-20	22.5	4.02
D 10-50-25 P 8-10-20	22.5	10.7

The following procedure is used to quantify the cytotoxic effect of dextran:PEG degradation products on vSMC:

1. Obtain 2 cryovials of second passage vSMC from storage. Use standard plating procedure to plate each vial onto a P10 culture plate.

2. Prepare the 8 selected dextran:PEG material formulations (Table 5). Use a silicon mold to cast a (8 mm diameter, 3 mm thick) disk of each material variation.

3. Suspend each disk in a scintillation vial in 20 ml Dubelco's modified eagle medium (DMEM, 1X glucose) to promote material degradation. Keep at room temperature.

4. Immediately following start of material suspension, sterilize vials (and contents) with 4 hours exposure to UV light under culture hood.

5. After cell cultures reach confluence, passage onto ten 12 well plates (1:5 passage expansion).

6. Incubate wells until approximately 50% confluent. At this point, conduct cell counting on well 1 of five selected plates.

7. At 50% confluence, replace the media in each of the wells with a 1:1 mixture of media and material suspension supernatant (1 ml of each, 2 ml total volume per well). In this co-culture, material degradation products have developed over a 7 day period, and the degradation supernatant is termed the early degradation products.

8. Incubate the co-culture for 24 hours.

9. Following 24 hour incubation period, conduct cell counting and cytotoxicity assays.

10. Repeat the above steps (1-9) again with the same materials following a 21 day material degradation period. The degradation supernatant is now termed the late degradation products.

11. Record and analyze cytotoxicity data with Excel software.

Culture treatments

1. DMEM control – Cells cultured initially in normal media, but at 50% confluence media was replaced with 50% media + 50% DMEM (for final 24 hour incubation).

2. Fully lysed – Cells cultured in normal media for the entire duration of the experiment. Lysis buffer applied to culture prior to cutotoxicity assay in order to form the basis for a data transform into a relative cytotoxicity.

3. Material samples – Cells cultured in normal media until 50% confluent, at which point the normal media is replaced with (50% normal media + 50% degraded sample supernatant) for 24 hour co-culture incubation.

Cytotoxicity assay description

A cytotoxicity assay kit (Vybrant^{TM}, V-2311) was used to quantify the concentration of the cytosolic enzyme glucose 6-phosphate dehydrogenase (G6PD) in cell culture supernatant. The release of this enzyme by cells is indicative of cell damage or death. The cytotoxic levels (G6PD concentrations) of cell populations subject to various treatments are converted to a relative cytotoxicity by means of comparison to a lysis control, which gives the G6PD level for a totally dead cell population of known size. A Multisizer 3 Coulter Counter (Beckman Coulter) was used to count cells populations in 12-well plates following various culture treatments. The cell counts form the basis for adjusting the relative cytotoxicity measurements to account for well density.

Calculation of adjusted relative cytotoxicity

The adjusted relative cytotoxicity considers both the size (cell density) and the health (relative cytotoxicity) of cell cultures after exposure to dextran:PEG degradation products. The

adjusted relative cytotoxicity is interpreted as a rating of cell culture health in this study, and is calculated as follows:

$$\text{Adjusted Relative Cytotoxicity} = (\text{Relative Cytotoxicity}) / (\text{Cell Density})$$

3.4.2 Proliferative Effect of Polymerized Dextran:PEG Materials

Hypothesis

When dextran:PEG is polymerized directly on a cell monolayer, the ensuing material reactivity with cells will be dependent on the concentration of free aldehyde groups in the material.

Experimental objectives

Examine the proliferative effects of dextran:PEG materials applied to 3T3 fibroblast cells (mouse source). Compare the proliferation of 3T3 cells in the presence of selected dextran:PEG materials (Table 6). The materials formulated for proliferative analyses span a wide range of reactive group ratio (1.29 - 7.22) with relatively small variance in total solid content (25 % - 35 %).

Table 6: Dextran:PEG samples prepared for cell proliferation testing

Sample Label	Total Solid Content (%)	CHO:NH$_2$
D10-20-20 P10-8-50	35	1.29
D10-20-20 P10-8-40	30	1.61
D10-20-20 P10-8-32	26	2.01
D10-50-14 P10-8-40	27	3.00
D10-50-18 P10-8-32	25	4.82
D10-50-27 P10-8-40	29	5.78
D10-50-27 P10-8-32	29.5	7.22

Experimental procedures

The following procedure is used to quantify the effect of polymerized dextran:PEG materials on fibroblast proliferation:

1. Culture 3T3 cells to approximately 50% confluence in 12-well plates.
2. Aspirate media from each well plate.
3. Add 0.25 ml (single drop from 12-step mixing tip) of formulated dextran:PEG (Table 6) to each well plate (follow same material sterilization procedure as cytotoxicity assay, Section 3.4.1).
4. Add 1 ml media to each well plate
5. Incubate (cells + materials) for 24 hours.
6. Following co-culture, conduct proliferation assay on all well plates.
7. Record and analyze proliferation data with Excel software.

Culture treatments

1. Media control – Cells cultured in normal media throughout duration of the experiment. No dextran:PEG materials were applied to culture prior to performance of proliferation assay.

2. Material control – Proliferation assays were conducted on wells with dextran:PEG materials but without any cells. The chemical effect of each material on the assay reagents was examined with these controls, and was taken into account in the interpretation of cell proliferative measurements.

3. Material samples – Cells were grown in 12-well plates in accordance with normal culture protocol until approximately 50% confluent. At this point, 0.25 ml of dextran:PEG was polymerized on the cell layer, and the cells + material were co-cultured for 24 hours.

Proliferation assay description

A colorimetric (MTT) assay (Chemicon®, CT02) was used to quantify the proliferation of 3T3 fibroblast cells following various culture treatments. The assay is based on absorbance measurements designed to detect the cleavage of MTT (3-(4, 5-dimethylthiazol-2-yl)-2,5-

diphenyl tetrasodium bromide), a process which requires mitochondrial activity. The MTT assay provides precise measurements of cell populations, as mitochondrial activity ceases rapidly following cell death.

Chapter 4: Results and Analyses

Chapter 4 details the results and analyses of hydration and degradation studies (Section 4.1), uniaxial tensile testing (Section 4.2), adhesion strength testing (Section 4.3), and in-vitro cell studies (Section 4.4). The chapter concludes with a preliminary compositional optimization of dextran:PEG copolymers for an adhesive sealant application (Section 4.5).

4.1 Swelling Ratio and Catastrophic Degradation Time

Dextran:PEG material suspensions were analyzed with a gravimetric technique described in Section 3.1. The analyses were conducted until disk fragmentation due to extensive polymer degradation prevented sample handling. Two material properties were extracted from each gravimetric analysis: the maximal swelling ratio and the onset of catastrophic material degradation.

The maximal swelling ratio reflects the highest mass increase measured for a disk throughout the suspension period. The swelling ratio indicates the hydration state of the dextran:PEG material, and is calculated as follows:

$$\text{Swelling Ratio}\,(\%) = \left[\frac{W_\infty - W_D}{W_D} \right] \times 100$$

where W_∞ is the maximal disk mass measured throughout the suspension period and W_D is the initial disk mass prior to suspension (dry sample).

The onset of catastrophic material degradation is defined as the time at which the suspended disk begins to lose net mass. At the point of catastrophic degradation, the extent of material loss due to hydrolytic network degradation exceeds the mass acquired via swelling. Although the dextran:PEG networks likely undergo near immediate hydrolytic degradation in aqueous suspension, slow degradation rates allow for significant water uptake and material persistence prior to loss of swollen polymer mass.

Figure 14 is a representative plot of the gravimetric data acquired for dextran:PEG disk suspensions (sample disk D 10-50-14 P 8-10-40, initial mass 0.342 g). The error bars in the graph denote ± 1 standard error of measurement for the sample disk mass (number of measurements = 3). The sample suspension was maintained for 96 hours, with a maximal mass of 3.26 g measured at the 54 hour time point. The maximal swelling ratio for this sample is calculated as 853.2 % and the onset of catastrophic degradation is 54 hours. At 96 hours, the sample disk has fragmented, preventing further gravimetric analysis.
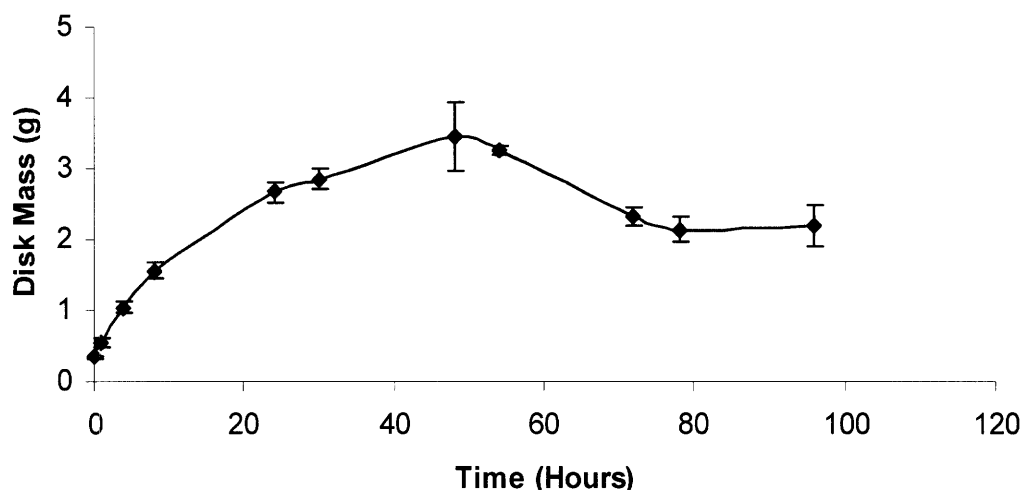
Figure 14: Representative data from gravimetric analyses (D 10-50-14 P 8-10-40)

The gravimetric data of dextran:PEG polymers is summarized in Table 7. The negative swelling ratio for D 10-50-7 P 2-2-50 indicates that this material underwent catastrophic degradation prior to the first measurement (1 hour). The swelling ratios and catastrophic degradation times for the analyzed materials ranged from -37.3 % to 926.7 % and 0.6 hours to 54 hours, respectively.

Table 7: Gravimetric data for dextran:PEG materials

Gravimetric Analyses	Swelling Ratio (%)		Onset of Catastrophic Degradation (hours)	
Sample	Average	Standard Deviation	Average	Standard Deviation
D 10-50-7 P 2-2-50	-37.3	6.0	0.6	0.0
D 10-50-20 P 2-2-50	80.2	9.1	4.7	1.7
D 10-50-45 P 2-2-30	89.0	7.8	6.7	2.3
D 10-50-25 P 2-2-50	95.8	24.1	4.0	0.0
D 60-20-25 P 2-2-30	10.0	2.3	2.0	0.0
D 40-25-25 P 8-10-10	182.1	16.3	8.0	0.0
D 10-50-25 P 8-10-21	621.7	49.8	50.0	3.5
D 10-50-5 P 8-10-40	231.7	76.9	32.3	11.6
D 60-20-15 P 8-10-38	492.6	126.2	46.0	13.9
D 10-50-14 P 8-10-40	926.7	178.1	44.0	10.4
D 40-25-15 P 8-10-20	293.0	44.2	23.8	5.5
D 60-20-20 P 8-10-21	401.0	76.8	44.7	8.0
D 10-50-5 P 8-10-38	217.7	18.0	24.0	0.0
D 10-50-14 P 8-10-21	631.0	83.3	54.0	0.0

Careful inspection of the materials formulated for gravimetric analyses reveals that PEG arm number and molecular weight have complete covariance: all linear (2-arm) PEG have a molecular weight of 2 kDa and all star (8-arm) PEG have a molecular weight of 10 kDa. PEG molecular weight is not included as a dextran:PEG compositional variable in the data analysis due to the complete covariance with PEG arm number within the material design space. The decision to exclude PEG molecular weight, as opposed to PEG arm number, is based on the hypothesized dramatic influence of constituent molecular complexity on resultant network properties. Nevertheless, the conclusions following from this gravimetric data set must be considered in light of this underlying assumption. Once molecular synthesis of star PEG molecules with various molecular weight is achieved, experimentation will be conducted to verify that PEG shape, rather than size, is the stronger determinant of polymer network properties.

Correlation analyses between the gravimetric data and the compositional variables of dextran:PEG are presented in Table 8. As indicated by the highlighted small p-values, PEG arm number was the only compositional variable to correlate with the dextran:PEG swelling ratios

and catastrophic degradation times. In both cases, the correlation coefficients (.707 and .805) indicate a strong positive relationship between PEG arm number and these material properties.

Table 8: Correlation analyses of gravimetric data and compositional variables

Correlation Analyses		D_MW	D_OX	D_SC	P_ARM	P_SC
Swelling Ratio	Coefficient	-0.052	0.066	-0.176	0.707	-0.283
	p-value	0.86	0.822	0.547	0.005	0.328
Onset of Degradation	Coefficient	0.073	-0.305	-0.294	0.805	-0.35
	p-value	0.805	0.906	0.308	0.001	0.219

Figures 15 and 16 plot the gravimetric data for all dextran:PEG samples, with an organization intended to highlight the positive correlation to PEG arm number. The error bars in the figures denote +1 standard deviation of the gravimetric data (n=3). As seen in the graphs, the dextran:PEG materials featuring star PEG constituents (maroon bars) generally have much greater swelling ratios and prolonged degradation times as compared to the linear PEG alternative (blue bars). Due to the superior hydration properties, subsequent analyses are focused on the characterization and development of dextran:PEG materials featuring a star PEG constituent.
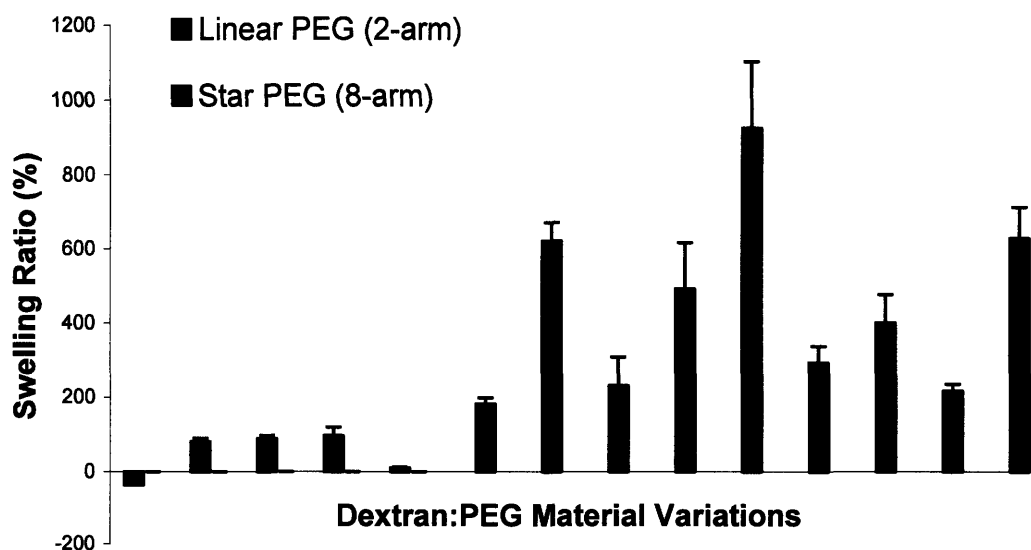
Figure 15: Influence of PEG arm number on material swelling ratio
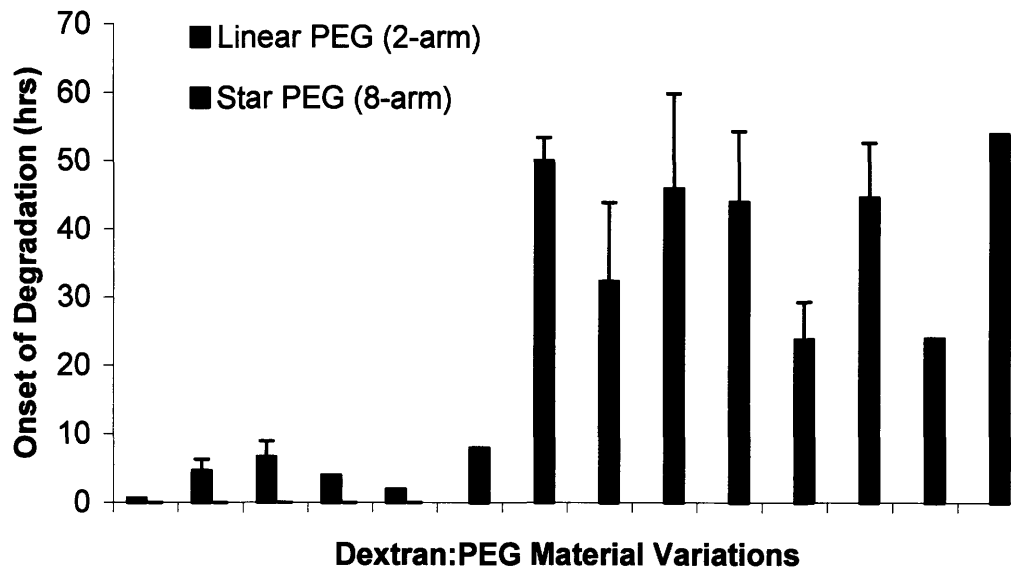
Figure 16: Influence of PEG arm number on catastrophic degradation time

Multiple linear regressions are used to model both the swelling ratio and catastrophic degradation times as functions of the compositional variables. The resulting regression equations are presented below, with the regressions detailed in Appendix A1. Each equation was developed with a regression p-value reduction scheme, with inclusion of only the compositional variables which accurately predict the gravimetric data [60]. In either case, PEG solid content was the only compositional variable removed from the regression model. The regression models can be used to roughly predict the swelling and degradation properties of any dextran:PEG compositional formulation, and provide a design tool for future material development.

Swelling Ratio (%) = - 2510 + 22.2(D_MW) + 40(D_OX) + 7.19(D_SC) + 89.7(P_ARM)

Onset of Degradation (hrs) = - 248 + 2.5(D_MW) + 4.08(D_OX) + 0.34(D_SC) + 7(P_ARM)

The recursive accuracies of the developed regression equations are verified in plots comparing the measured and modeled gravimetric data, as well as with Pearson's correlation

analyses. In Figure 17, the swelling ratio regression output is plotted against the corresponding data, with a resulting Pearson's correlation coefficient of 0.821 between modeled and measured values. A similar plot is presented for the catastrophic degradation times in Figure 18, with a Pearson's correlation of 0.935 between measured and modeled values. In both plots, the solid red line indicates perfect correlation between the modeled and experimental values, and is included as a visual aide.
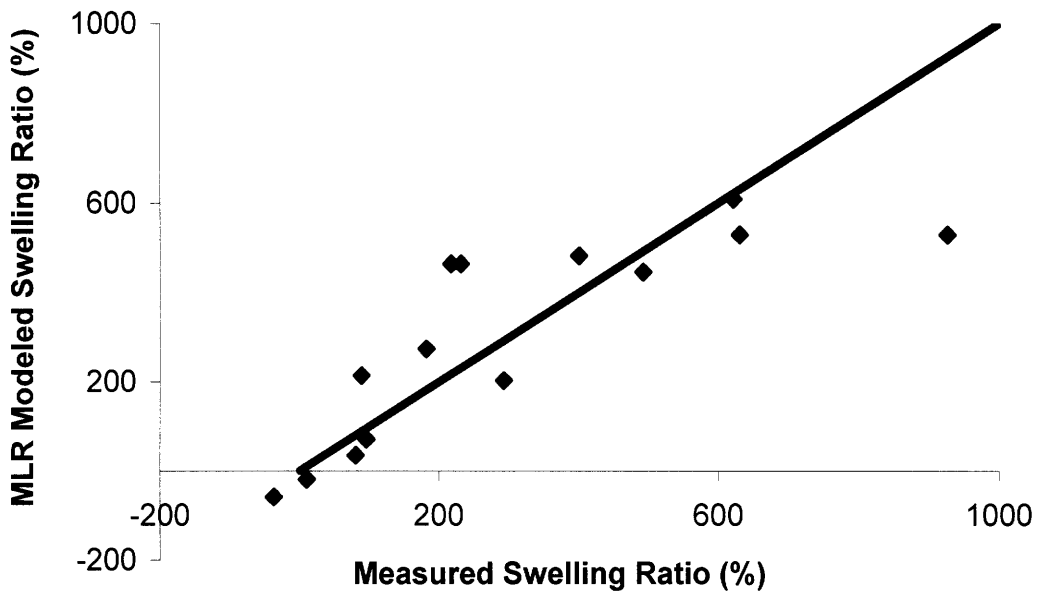
Figure 17: Comparison of MLR to swelling ratio data (Pearson's correlation = 0.821)
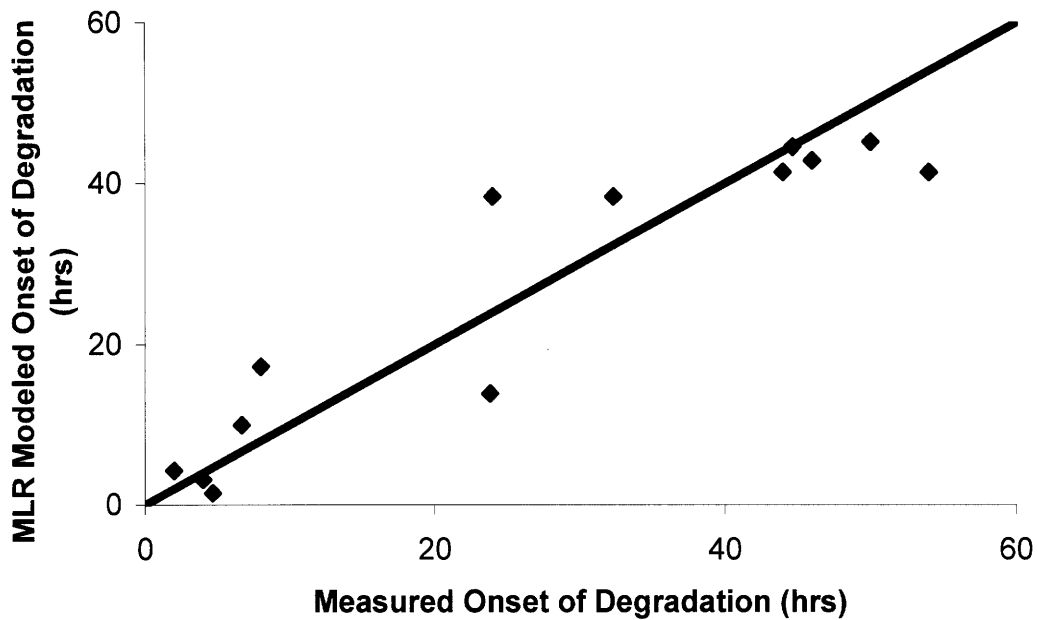
Figure 18: Comparison of MLR to onset of degradation data (Pearson's correlation = 0.935)

The number of arms in the constituent PEG is a highly deterministic predictor of both the swelling ratios and catastrophic degradation times of dextran:PEG polymers (Figures 15 and 16). Furthermore, correlation analyses between gravimetric data and PEG arm number indicates a similar dependence of these material properties on constituent PEG (Table 8). Since both properties (swelling ratio and catastrophic degradation time) depend on the same compositional variable (PEG arm number), a correlation is expected between the gravimetric data. As displayed in Figure 19, swelling ratio and catastrophic degradation time correlate well with each other, with a Pearson's correlation coefficient of 0.88. The solid line in Figure 19 is the linear regression between the gravimetric data, and is included as a visual aide.
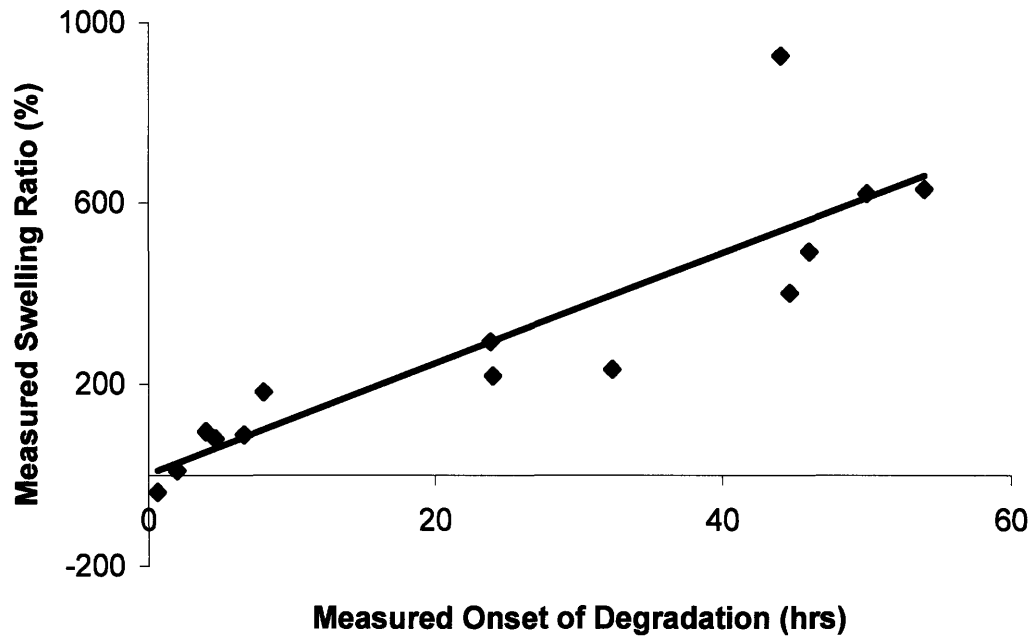
Figure 19: Relationship between gravimetric data (Pearson's correlation = 0.880)

4.2 Elastic Modulus

Uniaxial tensile testing data of dextran:PEG samples were processed to compute the elastic moduli of selected material formulations. The output of a uniaxial tensile test is force versus displacement data, which is transformed into true stress versus stretch ratio data as previously described (Section 3.2).

A plot of a representative dextran:PEG sample response to uniaxial extension is presented in Figure 20 (D 10-50-20 P 8-2-20). The error bars in the plot denote ± 1 standard error of measurement of repeated testing of the same sample (three runs per sample). The material sample was elongated to a stretch ratio of 1.12, which corresponds to a 12 % increase in length. The stress arising in the sample is seen to linearly increase with stretch ratio in this deformation regime. The slope of the linearized stress versus stretch ratio plot highlighted in red has the unit of Pascals, and is the sample elastic modulus.

Figure 20: Representative plot of uniaxial tensile testing data (D 10-50-20 P 8-2-20)

The measured elastic moduli for all tested dextran:PEG materials are tabulated below, along with the standard deviations of moduli between identical samples of each formulation (n=3). As seen in Table 9, the elastic moduli of examined dextran:PEG samples span an order of magnitude, ranging from approximately 30 – 300 kPa.
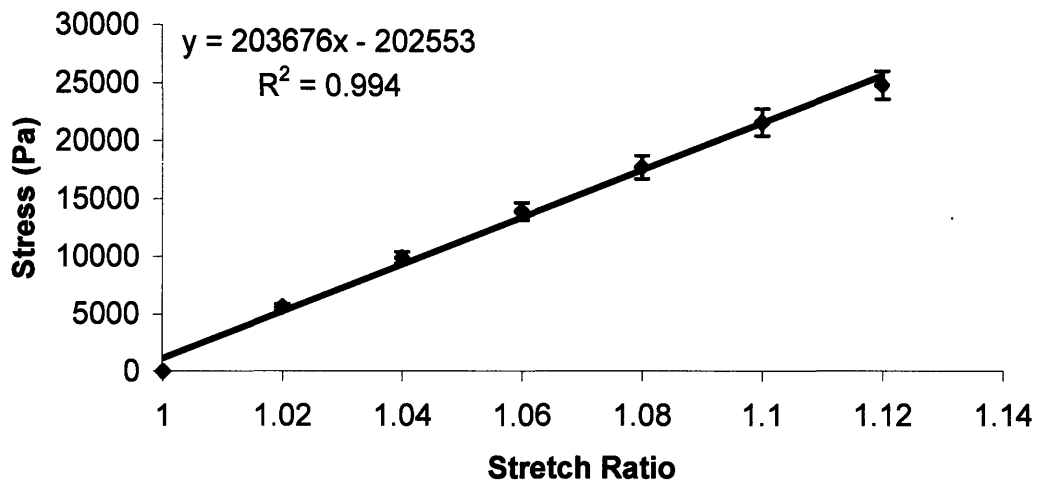
Table 9: Uniaxial tensile testing data for dextran:PEG materials

Uniaxial Tensile Testing	Elastic Modulus (Pa)	
Sample	Average	Standard Deviation
D 10-50-20 P 8-2-20	202375	16658
D 10-20-20 P 8-2-20	62901	557
D 60-20-20 P 8-2-20	86203	416
D 10-50-20 P 8-10-20	31859	250
D 10-20-20 P 8-10-20	61549	4009
D 60-20-20 P 8-10-20	65972	3639
D 10-20-40 P 8-2-20	258079	6707
D 10-20-40 P 8-10-20	63945	1632
D 10-20-20 P 8-10-60	195301	3107
D 60-20-20 P 8-10-60	207919	13114
D 10-50-20 P 8-10-60	316393	24633
D 10-20-40 P 8-10-60	258191	8465

A main effect analysis (see Figure 12 for schematic) is conducted to characterize the dextran:PEG stiffness response to compositional variation. The magnitude of the main effects serve as preliminary indicators of the importance of each compositional variable in determining the elastic modulus of dextran:PEG materials. A positive main effect indicates that increasing the compositional variable value will increase modulus, while a negative main effect indicates the opposite. Although design space limitations require careful interpretation of main effect analyses (further addressed in Section 5), compositional determinants of material properties can be identified in some obvious cases.

As seen in Table 10, the solid content of constituent PEG had an overwhelmingly large positive main effect on dextran:PEG elastic moduli when compared to the other compositional variables (+ 466.7 %). Dextran solid content and oxidation also have positive main effects on material modulus, confirming the expected effects of these compositional variations intuited in Section 2.2.2. The slight positive main effect of dextran molecular weight is unexpected, but the minimal magnitude suggests it is a weak determinant of dextran:PEG modulus. PEG molecular weight had a negative main effect on modulus, which can be understood through the tighter polymer network formed with a smaller PEG and the theory of rubber elasticity as earlier suggested.

Table 10: Main effects of compositional variation on dextran:PEG moduli

Compositional Variable	Dextran:PEG Main Effect (Pa)
Dextran Molecular Weight	12.8
Dextran Oxidation	71.4
Dextran Solid Content	82.1
PEG Molecular Weight	-55.6
PEG Solid Content	**466.7**

Similar to the approach taken to model the gravimetric data (Section 4.1), a multiple liner regression of the dextran:PEG elastic modulus response to compositional variation was developed. The resulting regression equation is presented below, and the details of the regression procedure are included in Appendix A1. All compositional variables except dextran molecular weight persist through model development, which along with the main effect analysis, further suggests the independence of dextran:PEG modulus on this compositional variable.

$$\text{Modulus (Pa)} = -82285 + 2341(\text{D\_OX}) + 4005(\text{D\_SC}) - 12070(\text{P\_MW}) + 4715(\text{P\_SC})$$

A plot of the modeled versus measured dextran:PEG moduli is presented in Figure 21. The solid red line in Figure 21 represents perfect correlation between the compared data, and is included as a visual aide. The regression model tracks well with the moduli data, with a Pearson's correlation coefficient of 0.908. The regression model provides a mathematical tool for design of dextran:PEG compositions of a target stiffness as well as informs on the molecular mechanisms governing network formation in these complex copolymers. However, the strength of the conclusions drawn from the regression analysis is also limited by the size of the material design space (12 material formulations) and the variation of dextran:PEG modulus with hydration time and temperature (Section 5).
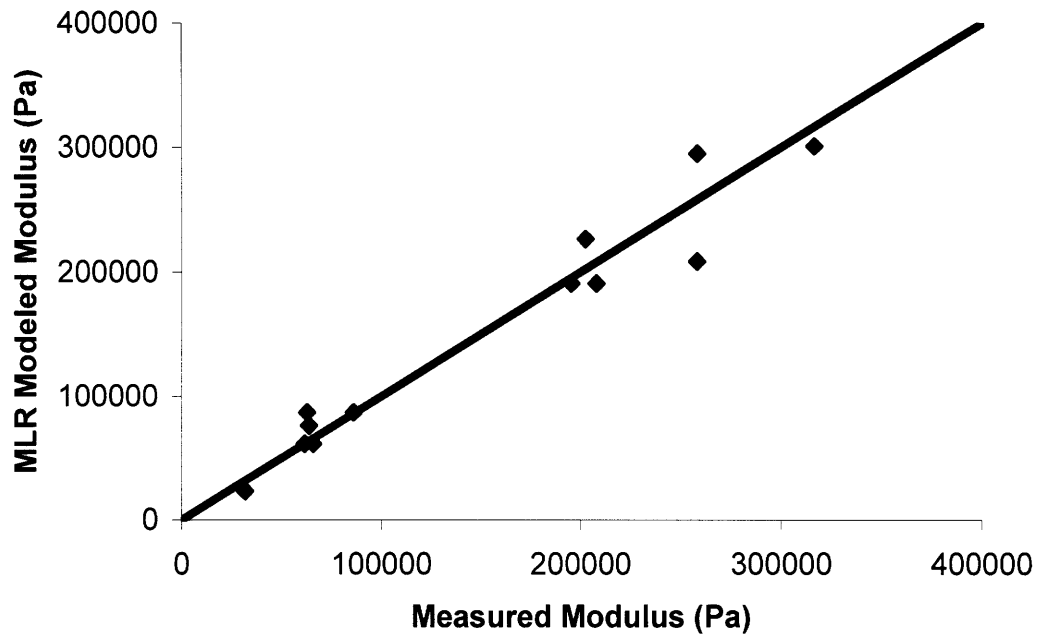
Figure 21: Comparison of MLR to elastic moduli data (Pearson's correlation =0.908)

4.3 Adhesion Strength

Interfaces between excised rat intestinal tissues and dextran:PEG materials were mechanically tested to rate the polymer bioadhesive strength. Tissue-material-tissue interfaces are subjected to a normal displacement at a constant rate as described in Section 3.3. The force required to disjoin the interface indicates the adhesive strength of the material.

The magnitudes of adhesion strength measured for dextran:PEG materials are invariably small due to the limited polymer volume applied to the interface (0.25 ml) and to the small interface contact area (less than 1 mm^2). The use of a high fidelity load cell and mechanical testing system allows for detection of sub-Newton forces, and facilitates differentiation of dextran:PEG adhesive strengths with the described testing parameters.

A representative plot of a tissue-material-tissue (D 10-50-20 P 8-2-20) interface displacement is shown in Figure 22. The initial displacement results in an increasing force that peaks around 0.054 N. The maximum (peak) force response to interface displacement is recorded as the sample adhesion force. After peaking, there is a quick drop in force as the tissue-material-tissue interface completely disjoins with additional displacement.

Figure 22: Representative data from adhesion strength testing (D 10-50-20 P 8-2-20)

The adhesion strengths measured for various dextran:PEG materials are displayed in Table 11, along with the standard deviations between three identical samples. As with elastic modulus, a large variance of this material property is seen amongst dextran:PEG formulations, with adhesion strengths spanning from near 0 to about 0.2 N. The span of property data promotes selection and design of dextran:PEG polymers for sealant applications. The magnitudes of bioadhesive strengths are expected to be much higher in-vivo, due to an increase of both polymer volume and tissue-material contact area as compared to the experimental setup.
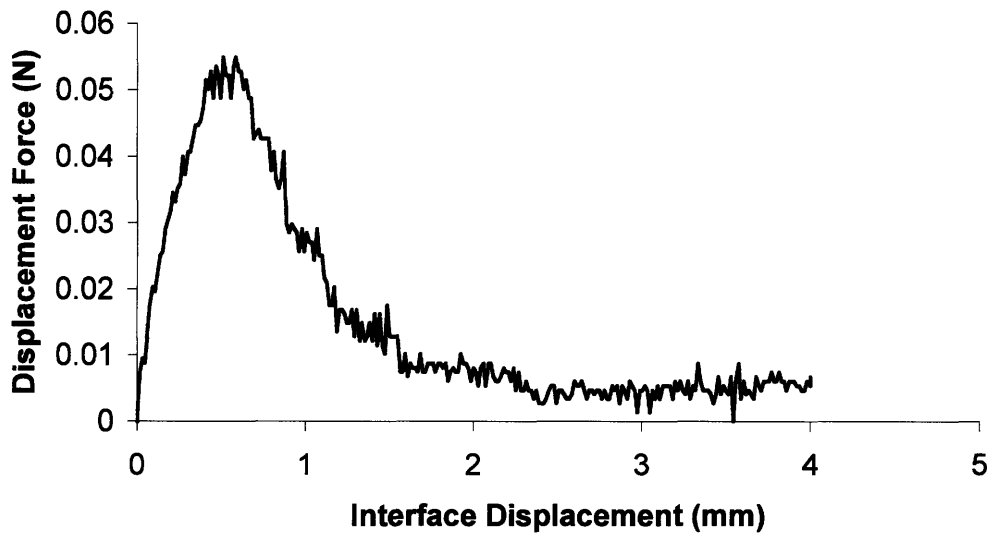
Table 11: Adhesion strength testing data for dextran:PEG materials

Adhesion Strength Testing	Adhesion Force (N)	
Sample	Average	Standard Deviation
D 10-20-20 P 8-2-20	0.056	0.022
D 60-20-20 P 8-2-20	0.112	0.041
D 10-20-20 P 8-10-20	0.008	0.002
D 60-20-20 P 8-10-20	0.021	0.001
D 10-20-20 P 8-10-60	0.057	0.007
D 60-20-20 P 8-10-60	0.020	0.007
D 10-50-20 P 8-2-20	0.110	0.049
D 10-50-20 P 8-10-20	0.124	0.009
D 10-50-20 P 8-10-60	0.145	0.036
D 10-20-40 P 8-10-20	0.190	0.053
D 10-20-40 P 8-2-20	0.125	0.035
D 10-20-40 P 8-10-60	0.108	0.032

A main effect analyses of the dextran:PEG adhesion force response to compositional variation is summarized in Table 12. The most deterministic variables of adhesion force are the constituent dextran oxidation and solid content. The positive main effects of these compositional variables on adhesion force are relatively large in magnitude, and are both related to the number of aldehyde groups in the dextran:PEG copolymers. Increasing either the dextran oxidation or solid content in a given material formulation will result in an increase in aldehyde content, provided all other compositional variables remain unaltered. Based on the main effect analyses, aldehyde reactivity with tissue is identified as the primary compositional determinant of dextran:PEG adhesion strength.

Table 12: Main effects of compositional variation on dextran:PEG adhesion strengths

Compositional Variation	Adhesion Force Main Effect (%)
Dextran Molecular Weight	26
Dextran Oxidation	**220**
Dextran Solid Content	**170.1**
PEG Molecular Weight	13.9
PEG Solid Content	-4.2

Comparatively small positive main effects were detected for molecular weight variations of both the dextran and PEG constituents (26 % and 13.9 %, respectively), weakly supporting the posited effect of polymer chain size on tissue-material reactivity (Section 2.2.2). Further bioadhesion testing with incremental variation of polymer chain size (as opposed to the binary low-high analyses presently used) is necessary for conclusive analyses of constituent molecular weight effects.

The small negative main effect (-4.2 %) of constituent PEG solid content on adhesion force indicates that PEG amine reactivity with tissue is minimal, and is at most a secondary adhesive mechanism to aldehyde reactivity. Additionally, studies of dextran:PEG polymerization rates show that increasing PEG solid content dramatically reduces the gel time of the tested materials, as seen in Figure 23. Accelerated gelling rates will limit the material spreading (and thus contact area) when polymerized on tissues. The associated decrease in gelling time and consequentially tissue-material contact area may explain the negative main effect of PEG solid content observed for dextran:PEG adhesion force.
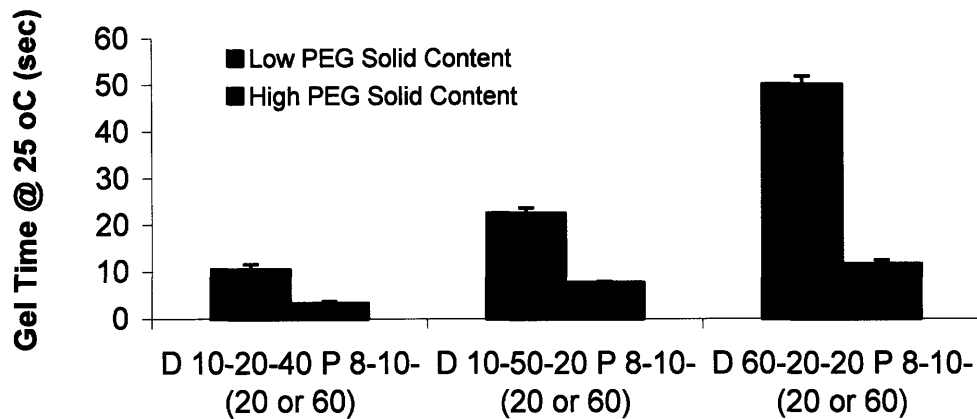
Figure 23: PEG solid content effect on dextran:PEG gel time

A multiple liner regression of the dextran:PEG adhesion force response to compositional variation was used to model the experimental data. The resulting regression equation is presented below, and the details of the regression procedure are included in Appendix A1. The only predictors remaining in the developed regression are the dextran oxidation and solid content, indicating a high dependency of dextran:PEG bioadhesion on these compositional variables.

$$\textbf{Adhesion Force (N)} = -0.103 + 0.00269(\textbf{D\_OX}) + 0.00477(\textbf{D\_SC})$$

A plot comparing the MLR model adhesion strengths and the experimental data is presented in Figure 24 below. The Pearson's correlation coefficient between the modeled response and the experimental data is 0.818, which is somewhat less accurate than other developed equations. As before, the red line in Figure 24 represents perfect correlation between the modeled and experimental values. The considerable error associated with the regression model suggest that the mechanisms of bioadhesion active in dextran:PEG copolymers are altered via interactive effects between compositional variables and/or nonlinear in nature with respect to the identified compositional determinants. The implicit error associated with all the developed regression models is further discussed in Section 5.
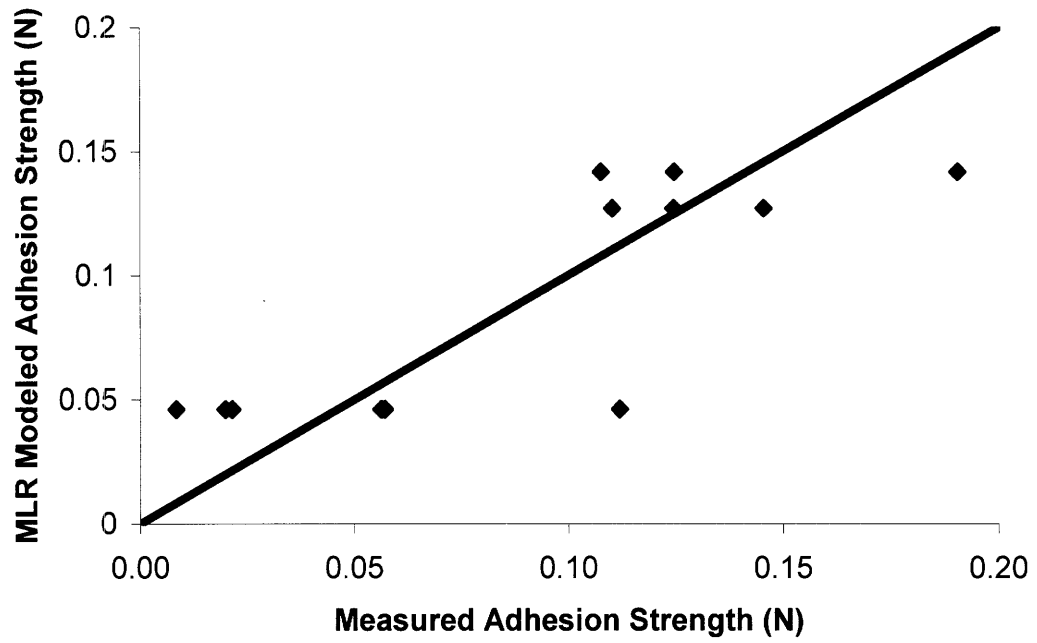
Figure 24: Comparison of MLR to adhesion strength data (Pearson's correlation =0.818)

4.4 Cytotoxicity and Proliferation

## 4.4.1 Cytotoxicity of Dextran:PEG Degradation Products

The adjusted relative cytotoxicities measured following smooth muscle cell exposure to dextran:PEG degradation products are listed in Table 13. Data from both the early and late degradation product exposures are included, along with a control DMEM sample (rates the cytotoxicity of the degradation medium). The tabulated standard deviations represent the data variance between identical sample treatments (n=3). In all cases, cellular exposure to pooled dextran:PEG degradation products results in elevated levels of adjusted relative cytotoxicity compared to the DMEM alone. The general increase in adjusted relative cytotoxicity between early and late degradation products of the same material suggests that extensive material degradation is required to instigate a cellular response.

Table 13: Cytotoxicity data for dextran:PEG degradation products

Cytotoxicity Testing	Early Degradation Cytotoxicity (G6PD release/cell x 10^6)		Late Degradation Cytotoxicity (G6PD release/cell x 10^6)	
Sample	Average	Standard Deviation	Average	Standard Deviation
DMEM Control	0.236	0.113	0.199	0.085
D 10-50-5 P 8-10-20	0.661	0.113	1.233	0.286
D 60-20-25 P 8-10-38	0.444	0.113	0.644	0.051
D 60-20-35 P 8-10-38	0.417	0.103	1.419	0.509
D 60-20-35 P 8-10-50	0.641	0.205	3.355	0.445
D 60-20-5 P 8-10-38	0.734	0.073	3.614	1.294
D 10-50-5 P 8-10-38	0.868	0.122	0.659	0.142
D 60-20-25 P 8-10-20	0.265	0.038	0.255	0.106
D 10-50-25 P 8-10-20	0.325	0.096	0.888	0.301

Figure 25 shows a subset of the adjusted relative cytotoxicity data selected to highlight the effect of total material solid content variation on the cellular response. The positive correlation expected between adjusted relative cytotoxicity and material solid content (Section 2.2.2) is largely supported by the data in Figure 25, with the exception of the cytotoxic effect of the low solid content material (D 10-50-5 P 8-10-20, total solid content = 12.5%). The unexpected level of adjusted relative cytotoxicity with a low solid content dextran:PEG is

understood through the degradation rates operative in these materials. Through visual inspection, it appeared that the low solid content material had completely dissolved following the 21 day suspension period, while other materials persisted to some extent proportional to the initial solid content. In other words, the supernatant of 12.5% solid content material suspension was likely more concentrated with by-product than expected when considering only initial solid content and ignoring degradation rates. The high level of cytotoxicity for the low solid content material variant is likely an artifact of by-product pooling as previously discussed. Positive correlation between solid content and adjusted relative cytotoxicity is still expected to persist, without exception, once the involved materials have all undergone complete degradation.
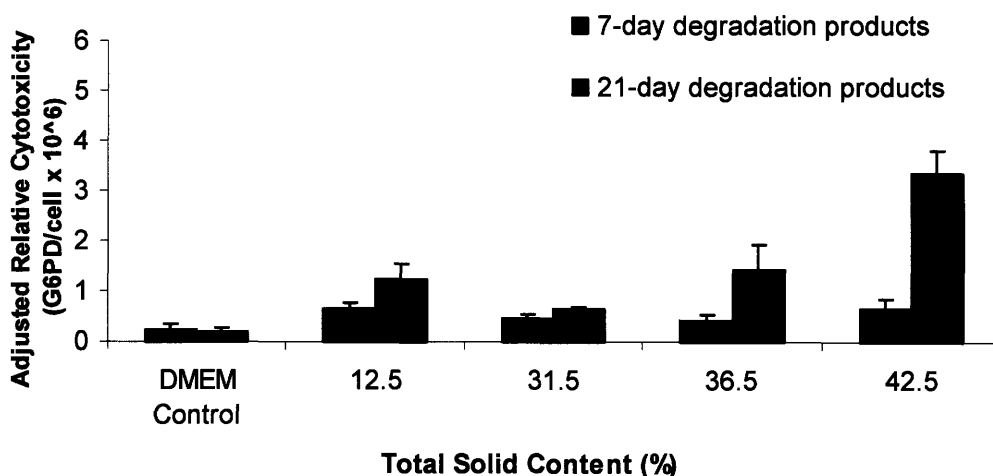
Figure 25: Effect of solid content on degradation-induced cytotoxicity

Figure 26 shows a subset of the adjusted relative cytotoxicity data, selected to highlight the effect of reactive group ratio variation. Material compositions with exceedingly high or low levels of $CHO:NH_2$ are relatively cytotoxic upon degradation. An intermediate reactive group ratio dextran:PEG material (D 60-20-25 P 8-10-20, $CHO:NH_2=4.02$) showed no statistically significant difference in cytotoxicity as compared to DMEM controls.
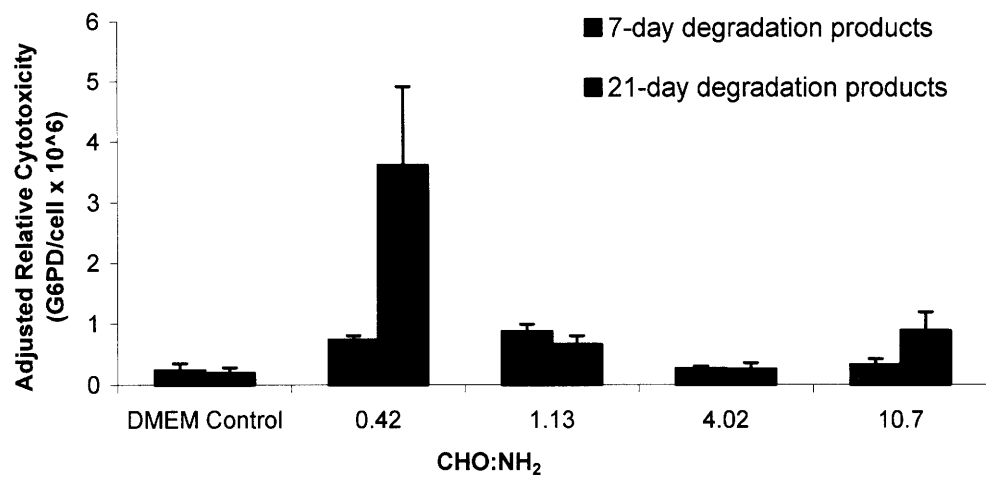
Figure 26: Effect of reactive group ratio on degradation-induced cytotoxicity

4.4.2 Proliferative Effect of Dextran:PEG Copolymers

The cellular response to direct applications of dextran:PEG polymers was studied with a colorimetric proliferation assay. Small volumes of various dextran:PEG materials were applied to uniform cultures of 3T3 fibroblast, which were subsequently incubated for 24 hours as described in Section 3.4.2. The cell numbers following incubation with the polymers indicates the material effects on cell proliferation.

The proliferation data for all tested dextran:PEG materials are displayed in Table 14. The extents of 3T3 proliferation in the presence of polymers are represented as a percent of control samples, to which no materials were applied. As indicated in Table 14, the cellular response to dextran:PEG polymers ranges from inhibition to stimulation of proliferation.

Table 14: Proliferation data for dextran:PEG copolymers

Proliferation Testing	3T3 Proliferation (% of Positive Control)	
Sample	Average	Standard Deviation
D 10-20-20 P 10-8-50	46.6	16.8
D 10-20-20 P 10-8-40	72.4	12.2
D 10-20-20 P 10-8-32	68.6	9.8
D 10-50-14 P 10-8-40	116.2	11.3
D 10-50-18 P 10-8-32	169.8	28.5
D 10-50-27 P 10-8-40	159.9	14.3
D 10-50-27 P 10-8-32	183.8	13.2

Figure 27 shows the proliferative effect of dextran:PEG polymers as a function of the material reactive group ratio. A positive trend is seen between reactive group ratio and cell proliferation, indicating that aldehyde reactivity with cells stimulates a proliferative response. As with the cytotoxicity studies (Section 4.4.1), the proliferation data suggests that dextran:PEG material formulations with intermediate reactive group ratios (2 - 3) are minimally reactive with cells in-vitro.
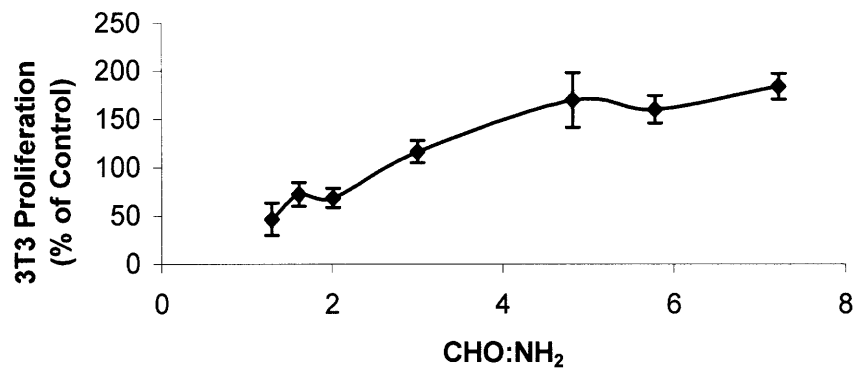
Figure 27: Effect of reactive group ratio on dextran:PEG-induced proliferation

4.5 Compositional Optimization

The gravimetric, mechanical and biological property data generated for dextran:PEG polymers are processed for preliminary optimization of material composition. The developed optimization procedure is targeted for selection of a candidate dextran:PEG material formulation for the model sealant application of small bowel resection. The optimization procedure is designed for compositional selection based on the following property criteria:

1. Relatively high dextran:PEG swelling ratio (biocompatibility)
2. Relatively long swelling time prior to onset of dextran:PEG catastrophic degradation (prolonged material functionality)
3. Dextran:PEG approximation of intestinal tissue stiffness (compliance matching)
4. Maximization of dextran:PEG adhesion strength (material functionality)
5. Relatively low dextran:PEG reactivity with cells (biocompatibility)

The observed enhancement of dextran:PEG swelling and degradation properties in materials including constituent star PEG (as opposed to liner PEG, Figures 15 and 16) are the first data utilized for compositional optimization. Based on the gravimetric data, the selected PEG arm number for optimal dextran:PEG formulation is eight, and linear PEG constituents are excluded from all other analyses.

The regression models of dextran:PEG mechanical data provide a quantitative means of compositional selection for targeted property criteria. In order to satisfy the corresponding property criteria, the regression equation for elastic modulus is minimized (as all tested dextran:PEG formulations are stiffer than intestinal tissue [61]) and the adhesion strength regression equation is maximized. Simultaneous minimization and maximization of the respective regression equations is easily accomplished with the Solver® function of Microsoft Excel.

The biological data describing the cytotoxic and proliferative effects of dextran:PEG polymers suggest a minimal level of cellular reactivity to intermediate reactive group ratio material formulations (Figures 26 and 27). Based on these data, boundary conditions of reactive

group ratio are placed on the aforementioned Solver® regression operations, with selection of the following bounds: $2.5 < CHO:NH_2 < 4.0$.

Figure 28 provides a schematic of the designed optimization procedure. As depicted, gravimetric, mechanical and biological property data all influence the compositional optimization.

6 Compositional Variables

PEG arm number

PEG mol. weight

PEG solid content

Dextran mol. weight

Dextran solid content

Dextran oxidation

Gravimetric Analysis

Select constituent star PEG

5 Compositional Variables

PEG mol. weight

PEG solid content

Dextran mol. weight

Dextran solid content

Dextran oxidation

Mechanical Testing

Biological Testing

MLR models

Boundary Conditions

Optimization of regression equations

Optimized dextran:PEG formulation

Figure 28: Schematic of dextran:PEG compositional optimization

The results of dextran:PEG compositional optimization are summarized in Table 15. For each compositional variable, the low and high variable columns refer to the minimum and maximum values synthesized to date, and are practical bounds of the optimization procedure. The additional bounds placed on polymer reactive group ratio also influence the optimization, although the effects are not readily evident in Table 15. The property metric is the target cell of the optimization script, and is the mathematical representation of simultaneous adjustment of modulus and adhesion strength regression equations. The actual value of the property metric is irrelevant to the optimization output, and is only included to aid in script visualization.

The column of optimized values in Table 15 lists the output of the optimization script. The optimized dextran:PEG formulation for the model adhesive sealant application is D 48-24-50 P 8-4-20, with a reactive group ratio of 4. Qualitatively, the optimized material has intermediate values of dextran molecular weight, dextran oxidation, and PEG molecular weight, a high dextran solid content, and a low PEG solid content. The optimization procedure outputs a candidate material for in-vivo studies of dextran:PEG polymers as adhesive sealants. The utility and limitations of the compositional optimization are further discussed in Section 5.

Table 15: Preliminary compositional optimization of dextran:PEG

Input			Output	
Compositional Variables	Variable Low	Variable High	Optimized Value	Property Metric
Dextran Molecular Weight	10	60	48.0	0.77
Dextran Oxidation	10	50	24.1	
Dextran Solid Content	10	60	50.0	
PEG Molecular Weight	2	10	4.1	
PEG Solid Content	20	60	20.0	

Chapter 5: Discussion

5.1 Implications and Limitations of Experimental Findings

The experimental data presented in this thesis are suggestive of compositional determinants of dextran:PEG polymer properties and provide insight into dominant molecular mechanisms governing the properties of interest. However, with the exception of the cellular response to material reactive group ratio, characteristic curves relating the compositional variables and material properties are lacking. Acquisition of characteristic curves for the six compositional variables and key material properties would require high throughput testing of dozens of dextran:PEG formulations. Complete analyses would also have to account for potential interactive effects between compositional variables, which would further expand the necessary design space.

The identified compositional determinants and preliminary dextran:PEG optimization presented in this thesis are limited by the underlying experimental design spaces. The data analyses implicitly assume that nonlinear effects of compositional variation and interactive effects between compositional variables are secondary phenomena to the described main effects. Instead of generating characteristic curves, the isolated low to high compositional variations forces a linear estimation of each material property response.

The use of incomplete material design spaces are justified by the purpose of the conducted experimentation. The data generated in this thesis are used to elucidate compositional determinants of material properties and suggest a candidate dextran:PEG material formulation for in-vivo testing. The entire data set generated for dextran:PEG materials can be viewed as preliminary with respect to future animal studies, as in-vivo data carries more clinical relevance for the usual reasons. Increasingly rigorous studies of compositional variation in-vitro will be conducted to test specific hypotheses rather than for basic material characterization. As the need arises for development of in-vitro characteristic curves in dextran:PEG, the current body of data provides a means for rational focus on particular compositional variables, namely the identified property determinants.

5.2 Effects of Hydration and Temperature

As polymers are heated or swell, there is typically an increase in network chain mobility and a corresponding loss of material stiffness. The mechanical compliance of a hydrophilic polymer implanted in-vivo is expected to increase as the material gradually becomes hydrated and heated to body temperature. Following dextran:PEG implantation, the modulus can be envisioned to relax in a manner similar to viscoelastic materials under constant displacement, with the driving force being increased swelling and temperature rather than mechanical loads.

A notable decrease in stiffness is seen as dextran:PEG materials swell over the course of a day. The stress responses to uniaxial deformation for a variably swollen dextran:PEG polymer (D 40-25-25 P 8-10-40, dog bone specimens as in Figure 11) is shown in Figure 29. Material samples were swollen in 100 ml aqueous medium for the indicated times prior to uniaxial tensile testing (mechanical testing procedure described in Section 3.2). As seen in Figure 29, increased hydration results in a dramatic decrease in dextran:PEG moduli (linear slope). The samples prepared for this study were hydrated via complete submersion in an aqueous medium. Although material hydration kinetics are expected to be much slower in an in-vivo environment, the variation of elastic modulus with implantation time should be considered in the design of sealants with particular stiffness (compliance-matched materials).
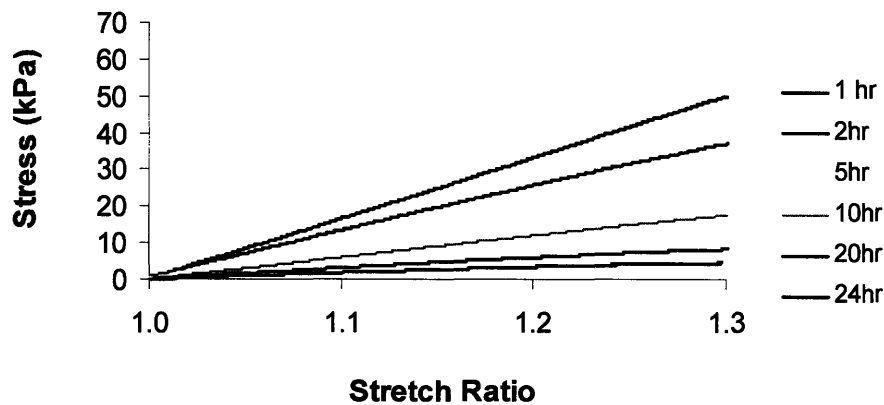
Figure 29: Dextran:PEG stiffness response to hydration

Due to the temporal nature of material swelling and the associated changes in polymer stiffness, the design of compliance-matched dextran:PEG sealants is complicated by considering *when* the tissue-material compliances should match with regards to implantation time. In-vivo models will be used to determine if it is more effective to match compliances at an early stage of implantation time (relatively low hydration), or alternatively match compliances after a given material implantation time (relatively high hydration). In either case, the developed modulus regression model can serve as a computational tool for compositional design of dextran:PEG.

5.3 Future Work

The inverse relationship between bioadhesion and biocompatibility (Figure 1) makes the development of adhesive sealants a scientifically interesting problem. Previous experience with available adhesive materials suggests that simply increasing material reactivity with tissue will indeed increase adhesion strength (cyanoacrylate-based sealants), but will also decrease biocompatibility. A scientific challenge facing adhesive sealant development is to devise a manner of independently adjusting these properties to design a high strength, biocompatible adhesive.

As demonstrated in this work, the compositional variance of dextran:PEG polymers facilitates design of targeted material properties. Furthermore, experimental evidence suggests that independent adjustment of adhesion strength and biocompatibility may be possible. For example, increasing the molecular weight of the copolymer constituent dextran has a positive main effect on adhesion strength, with no evident reduction in biocompatibility (reactive group ratio is a strong determinant of cell proliferation and cytotoxicity, and is independent of constituent dextran molecular weight).

It is hypothesized that long-chained flexible polymers with aldehyde groups throughout the chain length are able to react with cell-surface proteins to an extent similar to smaller aldehydes, resulting in highly adhesive materials. The long polymer chains of high molecular weight aldehydes may also improve biocompatibility, as less tissue penetration is envisioned to occur upon adherence and subsequent material degradation, analogous to the tissue response to glutaraldehyde-based fixation. Future work with dextran:PEG copolymers will explore such design strategies for adhesive sealant development.

Other avenues of dextran:PEG adhesive sealant development have been concurrently pursued with the presented work. For example, addition of controlled-release antibiotic cocktails into the polymer networks has been explored as a means to improve sealant clinical efficacy. The incorporation of antibiotics in the dextran:PEG necessarily modifies the polymer network, and the corresponding effects on other material properties (stiffness, adhesion strength) will have to be considered.

Following completion of in-vitro studies, the described small bowel resection model of an adhesive sealant application will be used to study dextran:PEG copolymers in-vivo. Correlation between in-vitro and in-vivo properties will be sought to rate the significance of material properties on clinical efficacy. The determined in-vitro-in-vivo correlations will be applied to the compositional design process, potentially resulting in an adhesive sealant with superior performance to currently available materials.

Chapter 6: Conclusion

Dextran:PEG polymers are a novel material class with potential for medical use as soft tissue adhesive sealants. The following property determinants relative to adhesive sealant applications have been identified for dextran:PEG materials:

1. Network complexity (PEG arm number) determines material hydration and catastrophic degradation time
2. Constituent PEG solid content determines elastic modulus
3. Aldehyde reactivity determines adhesion strength to tissue
4. Reactive group ratio determines material biocompatibility

Knowledge of the compositional determinants of key properties guides dextran:PEG development for adhesive applications, and provides understanding of the underlying molecular mechanisms active in these complex polymers. Future work will focus on in-vitro data correlation with in-vivo experimentation of dextran:PEG, as well as seek novel approaches to improve the state of the art of adhesive sealant technologies.

Appendix

A1: Summary of Regression Analyses

The following section provides a summary of the multiple linear regression analyses between dextran:PEG compositional variables and material properties. Each regression is represented with two consecutive figures in the following series (Figures 30-37). The first figure is a generally summary of the regression analysis, including the resulting regression equation and an analysis of variance. The second figure is a graphical representation of the regression residual analyses. All regression analyses were conducted with Minitab Software version 14.

Regression Analysis: Swelling Ratio versus D_MW, D_OX, D_SC, P_ARM, P_MW

```
* P_MW is highly correlated with other X variables
* P_MW has been removed from the equation.
```

The regression equation is
```
Swelling Ratio(%) = - 2510 + 22.2(D_MW) + 40(D_OX) + 7.19(D_SC)
                    + 89.7(P_ARM)
```

Predictor	Coef	SE Coef	T	P
Constant	-2510	1352	-1.86	0.096
D_MW	22.15	14.59	1.52	0.163
D_OX	39.98	23.00	1.74	0.116
D_SC	7.187	5.787	1.24	0.246
P_ARM	89.72	21.39	4.19	0.002

```
S = 191.164   R-Sq = 67.5%   R-Sq(adj) = 53.0%
```

Analysis of Variance

Source	DF	SS	MS	F	P
Regression	4	681938	170485	4.67	0.026
Residual Error	9	328892	36544		
Total	13	1010830			

Source	DF	Seq SS
D_MW	1	2722
D_OX	1	7712
D_SC	1	28906
P_ARM	1	642598

Unusual Observations

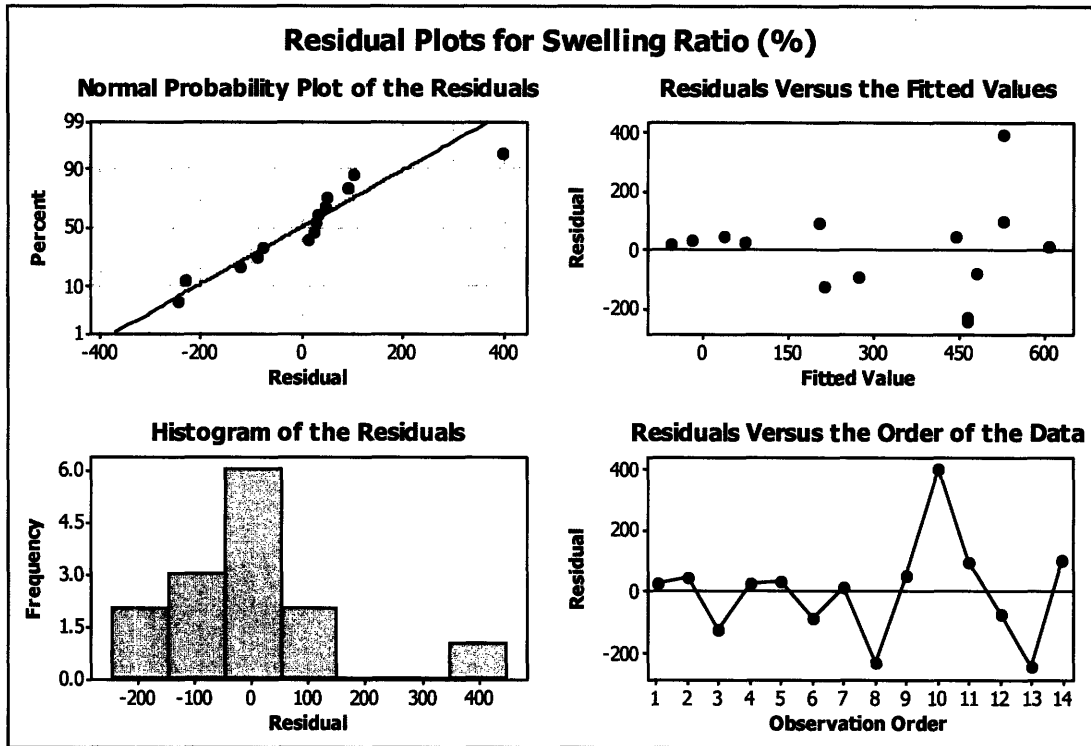| Obs	D_MW	Swelling Ratio (%)	Fit	SE Fit	Residual	St Resid
10	10.0	926.7	529.5	81.2	397.2	2.30R

Figure 30: Swelling ratio regression analysis summary

Figure 31: Residual plots for swelling ratio regression analysis

Regression Analysis: Onset of Degradation versus D_MW, D_OX, D_SC, P_ARM, P_MW

```
* P_MW is highly correlated with other X variables
* P_MW has been removed from the equation.
```

The regression equation is
```
Onset of Deg (Hrs) = - 248 + 2.47 D_MW + 4.08 D_OX + 0.340 D_SC
                          + 7.00 P_ARM
```

```
Predictor       Coef   SE Coef        T        P
Constant     -247.69     60.72    -4.08    0.003
D_MW          2.4690    0.6554     3.77    0.004
D_OX           4.082     1.033     3.95    0.003
D_SC          0.3399    0.2599     1.31    0.223
P_ARM         7.0001    0.9609     7.28    0.000
```

```
S = 8.58617   R-Sq = 87.5%   R-Sq(adj) = 82.0%
```

Analysis of Variance
```
Source              DF        SS        MS        F        P
Regression           4    4647.9    1162.0    15.76    0.000
Residual Error       9     663.5      73.7
Total               13    5311.4
```

```
Source    DF    Seq SS
D_MW       1      28.2
D_OX       1     241.3
D_SC       1     466.3
P_ARM      1    3912.1
```
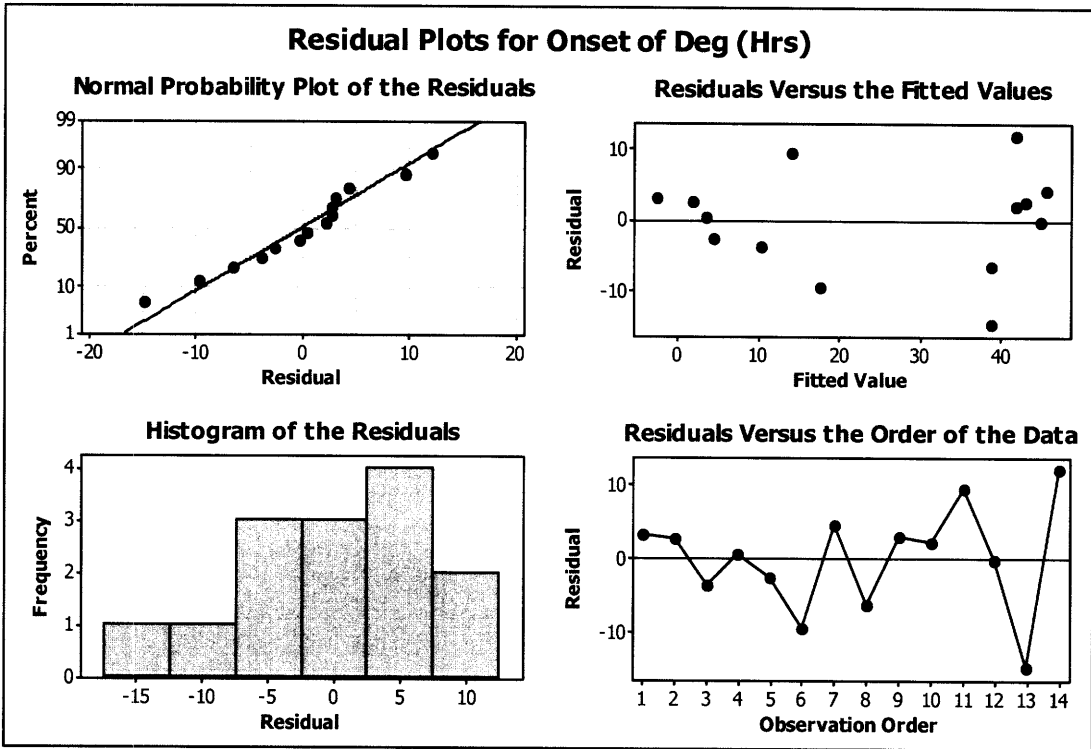
Figure 32: Onset of degradation regression analysis summary

Figure 33: Residual plots for onset of degradation regression analysis

```
Regression Analysis: Modulus (Pa) versus D_OX, D_SC, PEG_MW, PEG_SC

The regression equation is
Modulus(Pa) = - 82285 + 2341 D_OX + 4005 D_SC - 12070 PEG_MW +
4715 PEG_SC


Predictor      Coef   SE Coef        T       P
Constant     -82285     74342    -1.11   0.305
D_OX           2341      1223     1.91   0.097
D_SC           4005      1835     2.18   0.065
PEG_MW       -12070      4587    -2.63   0.034
PEG_SC       4715.5     917.4     5.14   0.001


S = 51896.4    R-Sq = 82.4%    R-Sq(adj) = 72.3%


Analysis of Variance
Source            DF            SS            MS      F       P
Regression         4   88264066812   22066016703   8.19   0.009
Residual Error     7   18852676583    2693239512
Total             11   1.07117E+11


Source    DF       Seq SS
D_OX       1    4264547112
D_SC       1   12831219012
PEG_MW     1      13480507
PEG_SC     1   71154820180
```
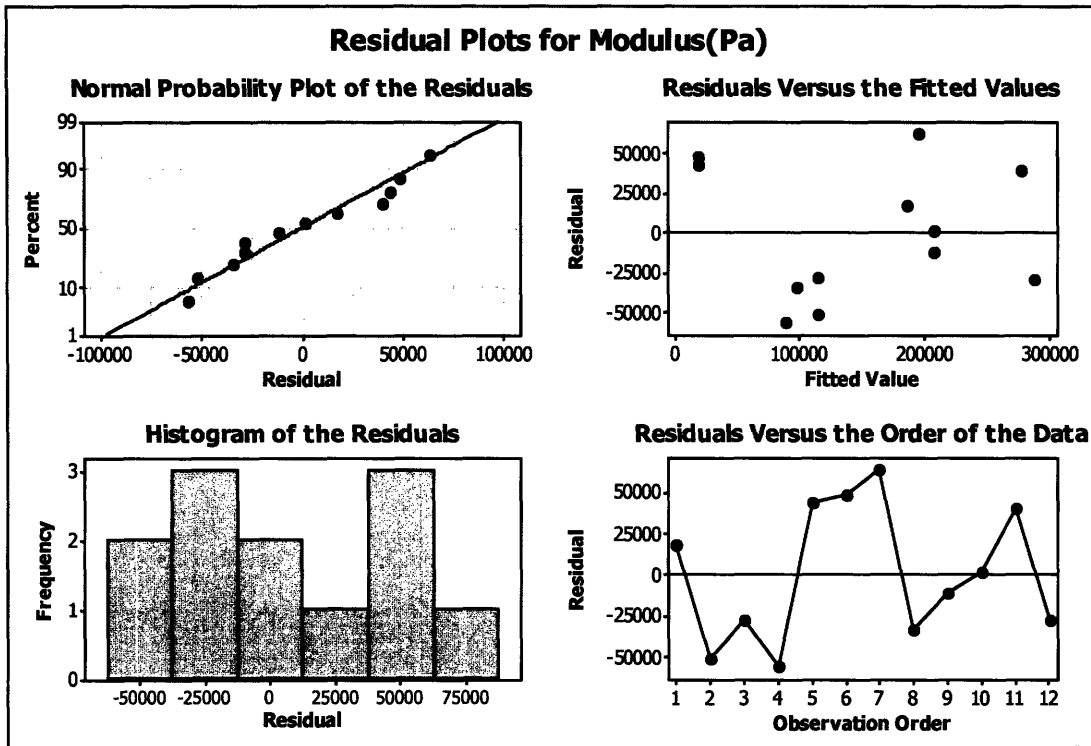
Figure 34: Modulus regression analysis summary

Figure 35: Residual plots for modulus regression analysis

Regression Analysis: Adhesion Force (N) versus D_OX, D_SC

The regression equation is
Adhesion Force (N) = - 0.103 + 0.00269 D_OX + 0.00477 D_SC

Predictor	Coef	SE Coef	T	P
Constant	-0.10344	0.04652	-2.22	0.053
D_OX	0.0026889	0.0008494	3.17	0.011
D_SC	0.004767	0.001274	3.74	0.005

S = 0.0360370   R-Sq = 66.8%   R-Sq(adj) = 59.5%

Analysis of Variance

Source	DF	SS	MS	F	P
Regression	2	0.023555	0.011777	9.07	0.007
Residual Error	9	0.011688	0.001299		
Total	11	0.035243			

Source	DF	Seq SS
D_OX	1	0.005378
D_SC	1	0.018177

Unusual Observations

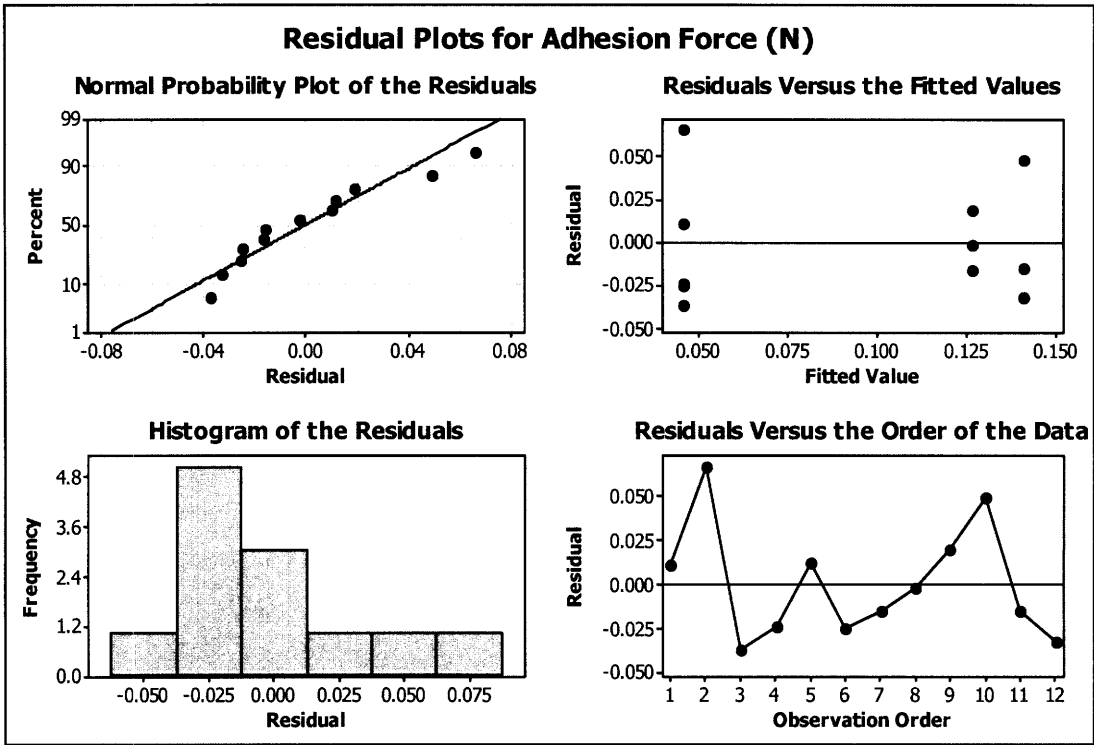| Obs	D_OX	Adhesion Force (N)	Fit	SE Fit	Residual	St Resid
2	20.0	0.1120	0.0457	0.0147	0.0663	2.02R

Figure 36: Adhesion force regression analysis summary

Figure 37: Residual plots for adhesion force regression

A2: Supportive Data for Cytotoxicity Study

Figure Organization

The effects of dextran:PEG degradation products on SMC cultures are graphically represented in a six figure series (Figures 38-43). Figures 38-40 describe the SMC response to co-cultures featuring material degradation products released after a 7 day suspension in DMEM, termed the early degradation products. Figures 41-43 describe the SMC response to co-cultures featuring material degradation products released after a 21 day suspension in the same medium, termed the late degradation products.

Each figure includes three bar graphs. The first bar graph displays the entire data set for a given assay. The second bar graph in each figure focuses on a portion of the data set selected to show the trend in cellular response as dextran:PEG solid content varies, and includes the first four samples listed in Table 5 (along with a DMEM control). Similarly, the third bar graph in each figure focuses on a portion of the data set selected to show the trend in cellular response as dextran:PEG reactive group ratio varies, and includes the second four samples listed in Table 5 (along with a DMEM control).

Figure Analysis

Figure 38 shows the relative cytotoxicity of various co-cultures featuring early degradation products. As emphasized in the third graph of Figure 38, the two low $CHO:NH_2$ dextran:PEG samples (D 10-50-5 P 8-10-38, $CHO:NH_2$ = 1.13 and D 60-20-5 P 8-10-38, CHO:NH2 = 0.42) have the most elevated cytotoxicity levels when compared to the DMEM control. The higher G6PD levels can be attributed to the extent of degradation in these materials after a 7 day suspension period, which was visibly greater than in any other of the formulations, presumably due to the low crosslinking density achieved in these material networks.

Figure 39 shows the cell density of various co-cultures featuring early degradation products. Once again, the co-culture involving a lightly crosslinked material (D 60-20-5 P 8-10-38, $CHO:NH_2$ = 0.42) showed the greatest effect on cell proliferation, which was significantly greater than the any other material formulation and the DMEM control.
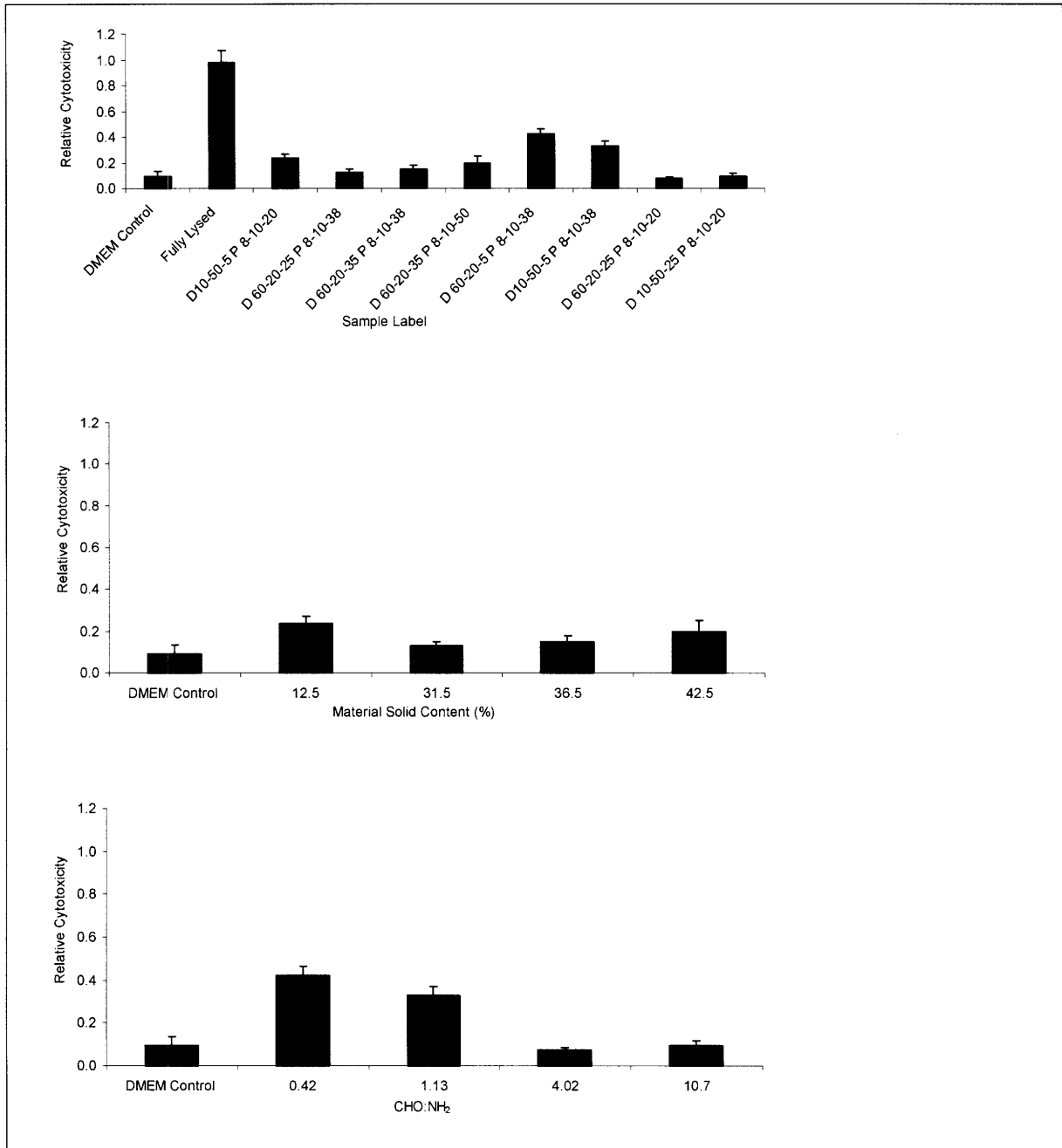
Figure 40 shows the adjusted relative cytotoxicity of various co-cultures featuring early degradation products. As shown in Figure 40, dextran:PEG material samples generally show elevated levels of adjusted relative cytotoxicity as compared to controls. No simple trend is sustained in adjusted relative cytotoxicity as material solid content is varied from high to low in Figure 40 chart 2, with high levels occurring at the highest (42.5 %) and lowest (12.5%) material solid contents. In either extreme of the solid content range, the cellular response can be attributed to the amount of material present in the degradation supernatant at the 7 day time point. In the high solid content material, the degradation supernatant should be relatively dense with material by virtue of the initial material density. However, the low solid content material also forms a relatively dense material supernatant, as the degradation rate will be faster than higher solid content alternatives. The same degradation rate-based logic can be used to understand the elevated levels of adjusted relative cytotoxicity observed for low $CHO:NH_2$, lightly crosslinked materials in the third graph in Figure 40.

Figures 41-43 present similar charts for the late degradation products data. Figure 41 shows the relative cytotoxicity of various co-cultures featuring late degradation products. As hypothesized, the relative cytotoxicity readings are in general greater in the late degradation products co-cultures as compared to the early degradation products. The solid content trend explored in Figure 41 chart 2 shows the expected positive correlation to cytotoxicity levels, with the exception of the lowest solid content formulation, which can again be attributed to the degradation rate. The third bar graph in Figure 41 captures the trend in cytotoxicity levels as $CHO:NH_2$ is varied, with a maximal response evidenced at ratio extremes (10.7 and 0.42). These data suggest that a material formulation featuring an intermediate $CHO:NH_2$ and solid content would inflict minimal cytotoxicity upon degradation.

Figure 42 shows the cell densities of various co-cultures featuring late degradation products. Little difference is noted between samples, although the cell densities are significantly depressed as compared to the DMEM controls.

Figure 43 shows the adjusted relative cytotoxicity of various co-cultures featuring late degradation products. Due the lack of sample differentiation with regards to cell densities, the
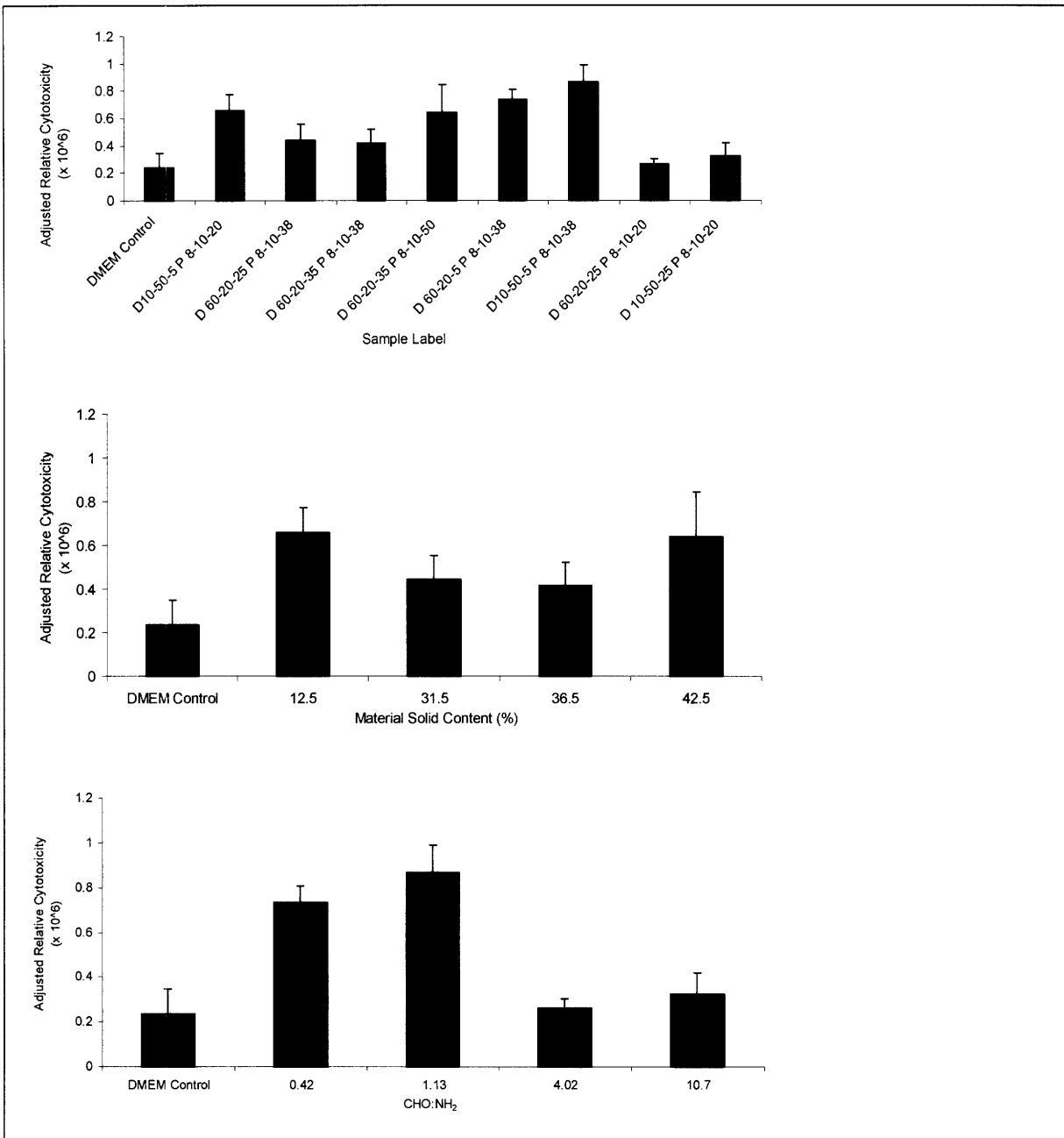
trends described for relative cytotoxicity (Figure 41) dominate this ratio and persist in the bar graphs of adjusted relative cytotoxicity for various dextran:PEG material formulations.
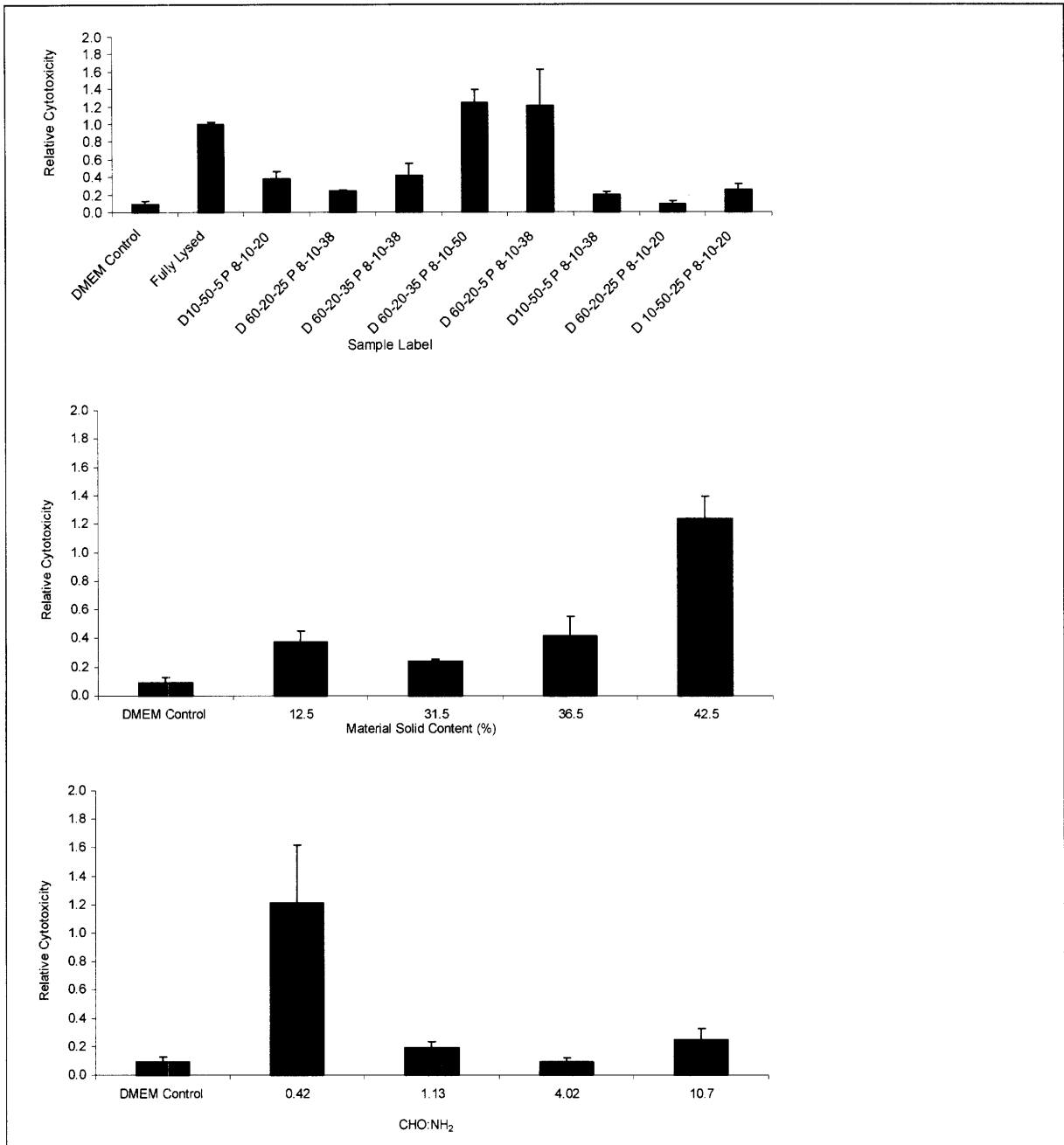

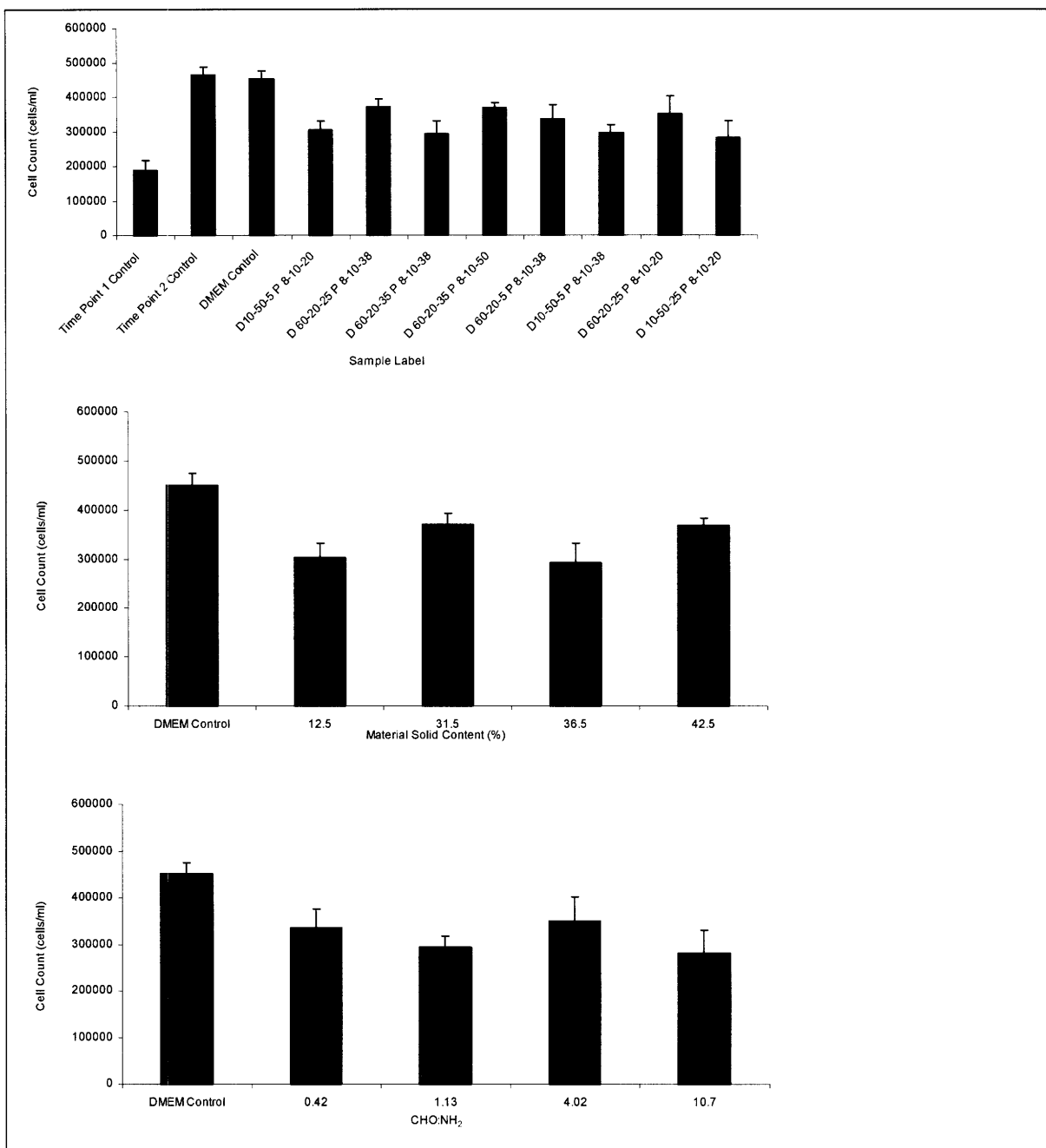Figure 38: Early degradation products cytotoxicity data
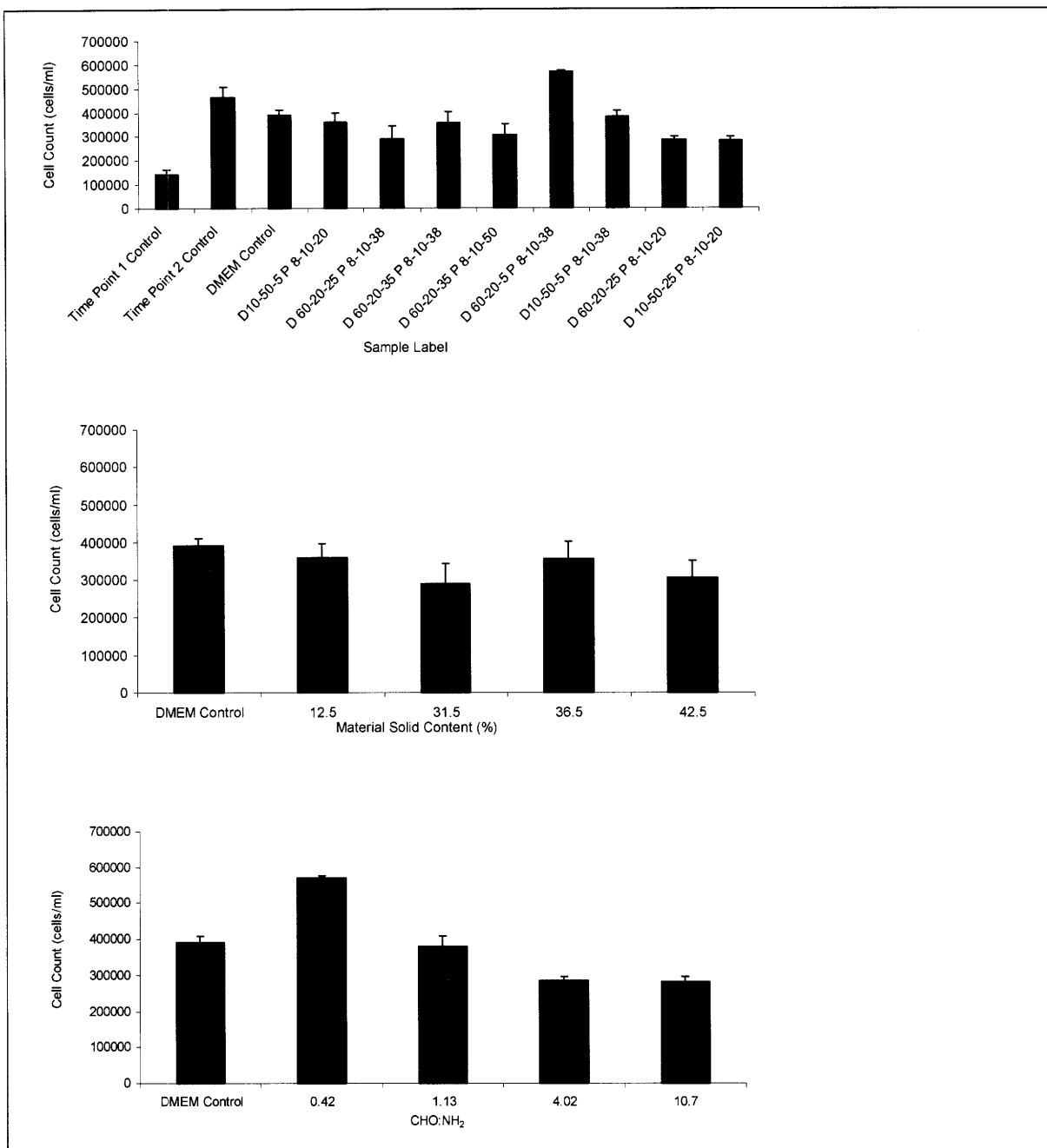
Figure 39: Early degradation products cell count data

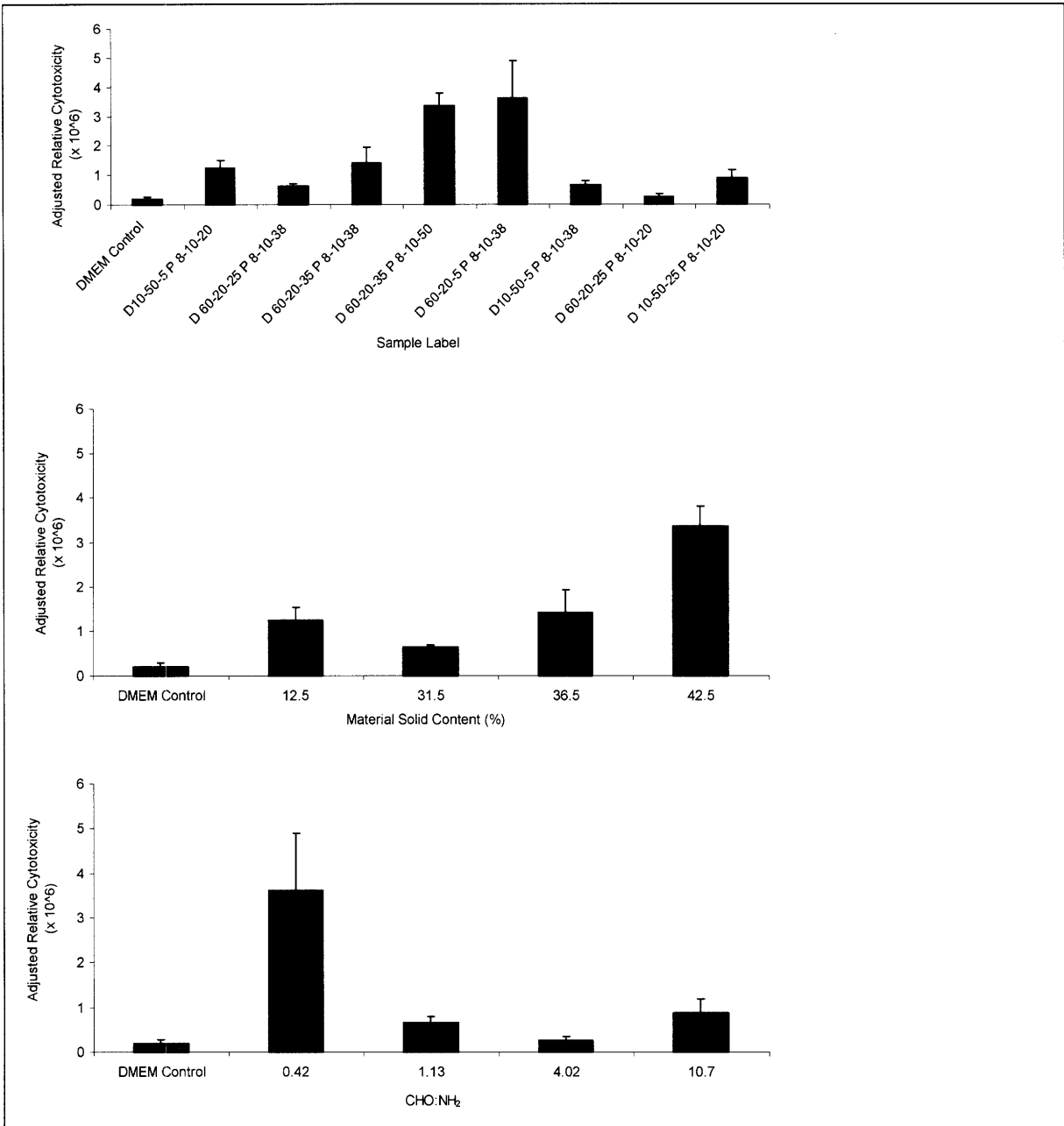**Figure 40: Adjusted relative cytotoxicity of early degradation products**

Figure 41: Late degradation products cytotoxicity data

Figure 42: Late degradation products cell count data

Figure 43: Adjusted relative cytotoxicity of late degradation products

Bibliography

1. Akgun, A., et al., *Early effects of fibrin sealant on colonic anastomosis in rats: an experimental and case-control study.* Tech Coloproctol, 2006. **10**(3): p. 208-14.
2. French, D.B. and R. Marcovich, *Fibrin sealant for retrograde ureteroscopic closure of urine leak after partial nephrectomy.* Urology, 2006. **67**(5): p. 1085 e1-3.
3. Everts, P.A., et al., *Platelet gel and fibrin sealant reduce allogeneic blood transfusions in total knee arthroplasty.* Acta Anaesthesiol Scand, 2006. **50**(5): p. 593-9.
4. Evans, L.A. and A.F. Morey, *Current applications of fibrin sealant in urologic surgery.* Int Braz J Urol, 2006. **32**(2): p. 131-41.
5. Sierra D., S.R., *Surgical Adhesives and Sealants.* 1996, Lancaster: Technomic Publishing AG.
6. Foster, J.A., et al., *Fibrin sealant for Muller muscle-conjunctiva resection ptosis repair.* Ophthal Plast Reconstr Surg, 2006. **22**(3): p. 184-7.
7. Lee, M.G. and D. Jones, *Applications of fibrin sealant in surgery.* Surg Innov, 2005. **12**(3): p. 203-13.
8. Salameh, J.R., J.H. Schwartz, and D.A. Hildebrandt, *Can LigaSure seal and divide the small bowel?* Am J Surg, 2006. **191**(6): p. 791-3.
9. Saygun, O., et al., *Reinforcement of the suture line with an ePTFE graft attached with histoacryl glue in duodenal trauma.* Can J Surg, 2006. **49**(2): p. 107-12.
10. Byrne, D.J., et al., *Adverse influence of fibrin sealant on the healing of high-risk sutured colonic anastomoses.* J R Coll Surg Edinb, 1992. **37**(6): p. 394-8.
11. van der Ham, A.C., et al., *Effect of fibrin sealant on the integrity of colonic anastomoses in rats with faecal peritonitis.* Eur J Surg, 1993. **159**(8): p. 425-32.
12. DeBono, R., *A simple, inexpensive method for precise application of cyanoacrylate tissue adhesive.* Plast Reconstr Surg, 1997. **100**(2): p. 447-50.
13. Toriumi, D.M. and A.A. Bagal, *Cyanoacrylate tissue adhesives for skin closure in the outpatient setting.* Otolaryngol Clin North Am, 2002. **35**(1): p. 103-18, vi-vii.
14. Toriumi, D.M., et al., *Use of octyl-2-cyanoacrylate for skin closure in facial plastic surgery.* Plast Reconstr Surg, 1998. **102**(6): p. 2209-19.
15. Toriumi, D.M., et al., *Histotoxicity of cyanoacrylate tissue adhesives. A comparative study.* Arch Otolaryngol Head Neck Surg, 1990. **116**(5): p. 546-50.
16. Kaplan, M. and K. Baysal, *In vitro toxicity test of ethyl 2-cyanoacrylate, a tissue adhesive used in cardiovascular surgery, by fibroblast cell culture method.* Heart Surg Forum, 2005. **8**(3): p. E169-72.
17. Coopersmith, C.M. and J.A. Lowell, *Surgery of the small intestine.* Curr Opin Gastroenterol, 1999. **15**(2): p. 146.
18. Gold, J.S. and R.P. Dematteo, *Combined surgical and molecular therapy: the gastrointestinal stromal tumor model.* Ann Surg, 2006. **244**(2): p. 176-84.
19. Stucchi, A.F., C.B. Aarons, and J.M. Becker, *Surgical approaches to cancer in patients who have inflammatory bowel disease.* Gastroenterol Clin North Am, 2006. **35**(3): p. 641-73.
20. Strong, S.A., *Surgical treatment of inflammatory bowel disease.* Curr Opin Gastroenterol, 2002. **18**(4): p. 441-6.

21. Fichera, A., et al., *Patterns and operative treatment of recurrent Crohn's disease: a prospective longitudinal study.* Surgery, 2006. **140**(4): p. 649-54.

22. Lepage, C., et al., *Incidence and Management of Primary Malignant Small Bowel Cancers: A Well-defined French Population Study.* Am J Gastroenterol, 2006.

23. Zanghi, G., et al., *[Stromal tumors of the small intestine: personal experience and review of the literature].* Ann Ital Chir, 2005. **76**(6): p. 549-52; discussion 552.

24. Ivatury, R.R., et al., *Complex duodenal injuries.* Surg Clin North Am, 1996. **76**(4): p. 797-812.

25. Margenthaler, J.A., et al., *Risk factors for adverse outcomes following surgery for small bowel obstruction.* Ann Surg, 2006. **243**(4): p. 456-64.

26. Demetriades, D., et al., *Penetrating colon injuries requiring resection: diversion or primary anastomosis? An AAST prospective multicenter study.* J Trauma, 2001. **50**(5): p. 765-75.

27. Cogbill, T.H., et al., *Conservative management of duodenal trauma: a multicenter perspective.* J Trauma, 1990. **30**(12): p. 1469-75.

28. Nasirkhan, M.U., et al., *Anastomotic disruption after large bowel resection.* World J Gastroenterol, 2006. **12**(16): p. 2497-504.

29. Bailey, A.A., et al., *Diagnosis and outcome of small bowel tumors found by capsule endoscopy: a three-center Australian experience.* Am J Gastroenterol, 2006. **101**(10): p. 2237-43.

30. Lipska, M.A., et al., *Anastomotic leakage after lower gastrointestinal anastomosis: men are at a higher risk.* ANZ J Surg, 2006. **76**(7): p. 579-85.

31. Houston, K.A. and O.D. Rotstein, *Fibrin sealant in high-risk colonic anastomoses.* Arch Surg, 1988. **123**(2): p. 230-4.

32. *The digestive system,* in *NIH Publication No. 06-5101,* National Institute of Diabetes and Digestive and Kidney Diseases.

33. Vander A., S.J., Luciano D., *Human Physiology-The Mechanicams of Body Function.* 2nd ed. 1975: McGraw-Hill, Inc.

34. *Anatomy of the Small Intestine,* in *Seer's Training Website, 2000 http://training.seer.cancer.gov/ss_module07_ugi/unit02_sec03_anatomy.html,* Seers.

35. Netter F., M.D., *Atlas of Human Anatomy.* 2000, East Hanover, New Jersey: Novartis.

36. Anderson, J., *Grant's Atlas of Anatomy.* 7th ed. 1978, Baltimore: The Williams and Wilkins Company.

37. Miller, G., et al., *Natural history of patients with adhesive small bowel obstruction.* Br J Surg, 2000. **87**(9): p. 1240-7.

38. *Intussusception,* in *Pathophysiology: Clinical concepts os disease processes, Price, S.A. and Wilson, L.Mc. 1992,* St Louis: Mosby-Year Book Inc. pg 318.

39. Lang, I. and E. Hitre, *[Current aspects of treatment in gastrointestinal stromal tumors (GIST)].* Orv Hetil, 2005. **146**(18 Suppl 1): p. 935-41.

40. *Histoogical display of Ulcer, Radiology Department of the University of Connecticut Health Center,* in *http://www.uchc.edu/,* University of Connecticut Health Center.

41. Downey, D.M., J.G. Harre, and J.P. Dolan, *Increased burst pressure in gastrointestinal staple-lines using reinforcement with a bioprosthetic material.* Obes Surg, 2005. **15**(10): p. 1379-83.

42. Kato, Y., et al., *Tissue adhesives for repairing inguinal hernia: a preliminary study.* J Laparoendosc Adv Surg Tech A, 2005. **15**(4): p. 424-8.

43. Geraghty, P.B., et al., *An investigation of the parameters influencing the bioadhesive properties of Myverol 18-99/water gels*. Biomaterials, 1997. **18**(1): p. 63-7.

44. Park, J.H. and Y.H. Bae, *Hydrogels based on poly(ethylene oxide) and poly(tetramethylene oxide) or poly(dimethyl siloxane): synthesis, characterization, in vitro protein adsorption and platelet adhesion*. Biomaterials, 2002. **23**(8): p. 1797-808.

45. Zhao, S.P., D. Ma, and L.M. Zhang, *New Semi-Interpenetrating Network Hydrogels: Synthesis, Characterization and Properties*. Macromol Biosci, 2006. **6**(6): p. 445-451.

46. Zhao, X., *Synthesis and characterization of a novel hyaluronic acid hydrogel*. J Biomater Sci Polym Ed, 2006. **17**(4): p. 419-33.

47. Arthur, S., *DuPont, Research Scientist*. 2007: Willmington, DE.

48. Anseth, K.S., C.N. Bowman, and L.B. Peppas, *Mechanical properties of hydrogels and their experimental determination*. Biomaterials, 1995. **17**(17): p. 1647.

49. Suggs, L.J., et al., *In vitro and in vivo degradation of poly(propylene fumarate-co-ethylene glycol) hydrogels*. J Biomed Mater Res, 1998. **42**(2): p. 312-20.

50. Tiwari, A., et al., *Improving the patency of vascular bypass grafts: the role of suture materials and surgical techniques on reducing anastomotic compliance mismatch*. Eur J Vasc Endovasc Surg, 2003. **25**(4): p. 287-95.

51. Teebken, O.E. and A. Haverich, *Tissue engineering of small diameter vascular grafts*. Eur J Vasc Endovasc Surg, 2002. **23**(6): p. 475-85.

52. Bratten, J.R. and M.P. Jones, *Small intestinal motility*. Curr Opin Gastroenterol, 2007. **23**(2): p. 127-33.

53. Wilson, D.J., et al., *Physical and biological properties of a novel siloxane adhesive for soft tissue applications*. J Biomater Sci Polym Ed, 2005. **16**(4): p. 449-72.

54. Sokolsky-Papkov, M., A.J. Domb, and J. Golenser, *Impact of aldehyde content on amphotericin B-dextran imine conjugate toxicity*. Biomacromolecules, 2006. **7**(5): p. 1529-35.

55. Draye, J.P., et al., *In vitro and in vivo biocompatibility of dextran dialdehyde cross-linked gelatin hydrogel films*. Biomaterials, 1998. **19**(18): p. 1677-87.

56. Park, H. and J.R. Robinson, *Mechanisms of mucoadhesion of poly(acrylic acid) hydrogels*. Pharm Res, 1987. **4**(6): p. 457-64.

57. Omidian, H., J.G. Rocca, and K. Park, *Elastic, superporous hydrogel hybrids of polyacrylamide and sodium alginate*. Macromol Biosci, 2006. **6**(9): p. 703-10.

58. Raman, A., *Materials selection and applications in mechanical engineering*. 2007, New York.

59. Suggs, L.J., et al., *In vitro cytotoxicity and in vivo biocompatibility of poly(propylene fumarate-co-ethylene glycol) hydrogels*. J Biomed Mater Res, 1999. **46**(1): p. 22-32.

60. Hayter, A., *Probability and Statistics*. 2nd ed. 2002, Pacific Grove, CA: Wadsworth Group.

61. Liao, D., et al., *The effect of epidermal growth factor on the incremental Young's moduli in the rat small intestine*. Med Eng Phys, 2003. **25**(5): p. 413-8.